

# Phenomenological Theory of Multiple Spin Density Waves in fcc Transition Metals

Takashi UCHIDA<sup>1\*</sup> and Yoshiro KAKEHASHI<sup>2</sup>

<sup>1</sup>*Hokkaido Institute of Technology, Maeda 7-15-4-1, Teine-ku, Sapporo 006-8585*

<sup>2</sup>*Department of Physics and Earth Sciences, Faculty of Science, University of Ryukyus, 1 Senbaru, Nishihara, Okinawa, 903-0213*

(Received May 10, 2018)

The relative stability among the multiple spin density wave (MSDW) states in fcc transition metals has been investigated on the basis of a Ginzburg-Landau type of free energy with terms up to the fourth order in magnetic moments. Obtained magnetic phase diagrams in the space of expansion coefficients indicate the possibility of various  $3\mathbf{Q}$  MSDW states in fcc transition metals: the commensurate  $3\hat{\mathbf{Q}}$  state with  $\hat{\mathbf{Q}} = 2\pi/a$  ( $a$  being the lattice constant), the incommensurate linearly polarized  $3\mathbf{Q}$  state, and the incommensurate helically polarized  $3\mathbf{Q}$  state. It is shown that these  $3\mathbf{Q}$  states are always stabilized, when they are compared with the corresponding  $2\mathbf{Q}$  and  $1\mathbf{Q}$  states, and their magnetic moment amplitudes are the largest among those of the three states. The results are compared with previous results of the ground-state calculations, and possible scenarios to explain the experimental data of cubic  $\gamma$ -Fe are proposed.

KEYWORDS: multiple spin density waves, linear spin density waves, helical spin density waves, fcc transition metals,  $\gamma$ -Fe, itinerant magnetism, magnetic structure

## 1. Introduction

Transition metals with nearly half-filled bands, such as Cr,<sup>1</sup> Mn,<sup>2-4</sup>  $\gamma$ -Fe,<sup>5,6</sup> and their alloys,<sup>7-12</sup> show complex magnetic structures due to competing magnetic interactions. The determination of their magnetic structures has long been a challenging problem in both theory and experiment in the study of metallic magnetism.<sup>13</sup> Of these, iron in the fcc phase ( $\gamma$ -Fe) has received special attention, since it is located at a crossover point from the ferromagnetic to the antiferromagnetic state on the periodic table and has been suggested to show spin density wave (SDW) states.

Early experimental data on  $\gamma$ -Fe precipitates on a Cu matrix<sup>14</sup> and the extrapolation from those on  $\gamma$ -FeMn alloys<sup>9</sup> suggested that bulk  $\gamma$ -Fe shows the first-kind antiferromagnetic (AF) structure with wave vector  $\hat{\mathbf{Q}} = (0, 0, 1)2\pi/a$ . Here  $a$  denotes the lattice constant. Later, the neutron diffraction measurements<sup>5</sup> on cubic  $\gamma$ -Fe<sub>100-x</sub>Co<sub>x</sub> ( $x < 4$ ) alloy precipitates in Cu showed magnetic satellite peaks at wave vector  $\mathbf{Q} = (0.1, 0, 1)2\pi/a$ . The magnetic structure was suggested to be a helical SDW, but was not determined precisely because of the high symmetry of the crystal structure. On the other hand, thin Fe films epitaxially grown on Cu were reported to show simple ferromagnetism<sup>15,16</sup> or the coexistence of a low-spin AF state and a high-spin ferromagnetic state,<sup>17-19</sup> depending on the film thickness. Recent studies<sup>6</sup> on Fe films suggested, however, that the fcc phase of Fe is formed only for film thicknesses of 5 to 11 monolayers and SDW is realized in these films.

Theoretically, the magnetic structure of bulk cubic  $\gamma$ -Fe was investigated intensively by means of the ground-state theories of electronic-structure calculations. In most of the calculations,<sup>20-26</sup> the  $1\mathbf{Q}$  helical SDW struc-

ture was assumed for the bulk cubic  $\gamma$ -Fe and the wave vector that minimizes the total energy was determined. The obtained wave vectors, however, are different among different theoretical approaches. The linear muffin-tin orbital (LMTO) calculations by Mryasov *et al.*<sup>20</sup> and the augmented spherical wave (ASW) calculations by Uhl *et al.*,<sup>21</sup> both based on the local density approximation (LDA), yielded ground-state wave vector  $\mathbf{Q} = (0, 0, 0.6)2\pi/a$  for lattice constant  $a = 6.8$  a.u. On the other hand, K rling and Ergon<sup>22</sup> performed the LMTO calculations using the generalized gradient approximation (GGA), and found the energy minimum at  $\mathbf{Q} = (0.5, 0, 1)2\pi/a$ . Furthermore, the recent full potential calculations suggest the possibility of other ground-state wave vectors. Bylander and Kleinman<sup>23-25</sup> performed full potential calculations using the ultrasoft pseudopotential and found the energy minimum at  $\mathbf{Q} = (0, 0, 0.55)2\pi/a$ . By means of a modified ASW method, Kn pffle *et al.*<sup>26</sup> found the energy minimum at  $\mathbf{Q} = (0.15, 0, 1)2\pi/a$  for lattice constant  $a \leq 6.75$  a.u. Although the wave vector obtained in their calculations is close to the experimental value, more recent ground-state calculations<sup>27</sup> based on the full potential augmented-plane-wave method, which accounts for more complex magnetic structures, show that the  $1\mathbf{Q}$  helical SDW is not the stable state of  $\gamma$ -Fe.

The possibility of magnetic structures other than the  $1\mathbf{Q}$  helical SDW has been suggested by Fujii *et al.*<sup>28</sup> on the basis of the LMTO calculations and the von Barth-Hedin potential. They compared the energies among the first-kind AF structure with  $\hat{\mathbf{Q}} = (1, 0, 0)2\pi/a$ , the commensurate  $2\hat{\mathbf{Q}}$  structure with  $\hat{\mathbf{Q}} = (1, 0, 0)2\pi/a$  and  $(0, 1, 0)2\pi/a$ , and the  $3\hat{\mathbf{Q}}$  structure with  $\hat{\mathbf{Q}} = (1, 0, 0)2\pi/a$ ,  $(0, 1, 0)2\pi/a$ , and  $(0, 0, 1)2\pi/a$ . They concluded that the  $3\hat{\mathbf{Q}}$  structure is the most stable at  $a =$

\*E-mail address: uchida@hit.ac.jp

6.8 a.u. (experimental lattice constant). Antropov and co-workers<sup>29,30</sup> compared the energies of various magnetic structures, including the structures obtained from the spin-dynamics calculations with 32 atoms in a unit cell. Using the GGA potential and the *spdf* basis, they claimed that the  $3\hat{Q}$  structure superposed with a helical SDW with  $\mathbf{Q} = (0, 0, 1/6)2\pi/a$  is the most stable for lattice constant  $a = 6.6$  a.u., although it is nearly degenerate with a noncollinear eight-atom structure and helical structure.

Kakehashi and coworkers<sup>31,32</sup> have recently developed a molecular-dynamics (MD) approach which automatically determines the magnetic structure in a given unit cell at a finite temperature. Applying the approach to  $\gamma$ -Fe with 500 atoms in a unit cell ( $5 \times 5 \times 5$  fcc lattice),<sup>32</sup> they found an incommensurate multiple spin density wave (MSDW) state whose principal terms consist of  $3\mathbf{Q}$  MSDW with  $\mathbf{Q} = (0.6, 0, 0)2\pi/a$ ,  $(0, 0.6, 0)2\pi/a$ , and  $(0, 0, 0.6)2\pi/a$ . Subsequently, they performed the ground-state electronic-structure calculations<sup>33</sup> on the basis of the first-principles tight-binding LMTO method and the GGA potentials. Comparing the energies of various magnetic structures, including the  $1\mathbf{Q}$  helical SDW and the MSDW found in the MD calculations, they concluded that the MSDW becomes the most stable state for lattice constants  $6.8 \leq a \leq 7.0$  a.u. More recently, Sjöstedt and Nordström<sup>27</sup> implemented density-functional calculations based on the alternative linearization of the full-potential augmented-plane-wave method. They compared various competing collinear and non-collinear magnetic structures: ferromagnetic, commensurate  $1\hat{Q}$ ,  $2\hat{Q}$ , and  $3\hat{Q}$  structures, and double-layered antiferromagnetic, as well as incommensurate helical structures. For lattice constant  $a = 6.82$  a.u., a collinear double-layered AF state was found to be the most stable structure.

The results of the ground-state calculations described above indicate that we have not yet obtained a solid conclusion as to the ground-state magnetic structure of cubic  $\gamma$ -Fe. In particular, no agreement between theory and experiment has yet been obtained. The discrepancy between theory and experiment can be ascribed to both sides. On the experimental side, the difficulty originates in the fact that the bulk  $\gamma$ -Fe is stable only at high temperatures above the Curie temperature of  $\alpha$ -Fe. At low temperatures,  $\gamma$ -Fe can be stabilized either in the form of small precipitates<sup>5</sup> in Cu or in thin Fe films<sup>6,15–19</sup> grown on Cu. Thus, it is a subtle problem whether or not the SDW structure observed at low temperatures is identical with that should be realized in bulk cubic  $\gamma$ -Fe. Furthermore, Tsunoda<sup>5</sup> emphasized in his detailed analyses that the  $1\mathbf{Q}$  helical SDW is one of possible structures with the same wave vector because of the high symmetry of the crystal structure of  $\gamma$ -Fe.

On the theoretical side, the discrepancy should partly be ascribed to the various approximation schemes of the potential used in the density-functional calculations. As stated above, the equilibrium wave vectors for the  $1\mathbf{Q}$  helical SDW predicted by the LDA calculations<sup>20,21</sup> are different from those predicted by the GGA calculations.<sup>22</sup> Similarly, the results of the atomic sphere approximation

calculations<sup>22</sup> are not in agreement with those of full-potential calculations.<sup>23–27</sup> Through these calculations, it has become clear that there are various local minimum states in  $\gamma$ -Fe that are close in energy.

In this situation, it is worthwhile to approach this problem from a phenomenological, but more general point of view so that one can gain useful information about possible magnetic structures of  $\gamma$ -Fe from only the symmetry of the system. The purpose of the present paper is to carry out such analysis by means of a Ginzburg-Landau type of theory and to clarify possible scenarios for the magnetic structure of  $\gamma$ -Fe from a phenomenological point of view. Since the observed magnetic moment<sup>14</sup> of  $\gamma$ -Fe and calculated ones<sup>28</sup> near the equilibrium volume are rather small ( $\lesssim 1\mu_B$ ), we will expand, in §2, a phenomenological free energy with respect to magnetic moments, and derive a general expression of free energy up to the fourth order. In §3 and 4, we discuss commensurate and incommensurate SDW structures, respectively, and obtain the magnetic phase diagrams in the space of expansion coefficients. The results of a preliminary analysis for this part have been published.<sup>34,35</sup> In the last section, we discuss possible scenarios for the magnetic structure of  $\gamma$ -Fe that are consistent with the present theory.

In contrast to the previous Landau type of phenomenological theories applied to the incommensurate  $1\mathbf{Q}$  SDWs and their harmonics in Cr<sup>36,37</sup> and those applied to the commensurate MSDWs in  $\gamma$ -Mn alloys,<sup>38</sup> the present phenomenological free energy allows for incommensurate MSDWs with both linear and helical polarizations, in addition to the commensurate MSDWs. In this respect, it should be emphasized that, so far, there has been no discussion about the possibility of helical MSDW states having the wave vectors found in the  $\gamma$ -FeCo precipitates in Cu, in spite of the fact that such MSDWs are also consistent with the experimental observation<sup>5</sup> of cubic  $\gamma$ -Fe.

In the present analysis, we have shown that each  $3\mathbf{Q}$  state becomes the most stable state among the corresponding  $1\mathbf{Q}$ ,  $2\mathbf{Q}$ , and  $3\mathbf{Q}$  states for both commensurate and incommensurate wave vectors. This relation leads to magnetic phase diagrams that indicate the possibility of various  $3\mathbf{Q}$  MSDW states in fcc transition metals, which are found to be consistent with the previous results: the commensurate  $3\hat{Q}$  state with  $\hat{Q} = 2\pi/a$  for lattice constants  $6.5 \leq a \leq 6.8$  a.u. in the ground-state calculations,<sup>28,33</sup> and the incommensurate linearly polarized  $3\mathbf{Q}$  state for  $a \geq 6.8$  a.u. in the MD calculations.<sup>33</sup> The phase diagram also suggests a possibility of the incommensurate helically polarized  $3\mathbf{Q}$  state, which has not yet been investigated in the ground-state calculations.

## 2. Phenomenological Free Energy

We consider a free energy expansion with respect to the local magnetic moments on the fcc lattice. Because the magnetic system in the absence of external magnetic fields has the time reversal symmetry, the free energy must include only even order terms with respect to magnetic moments. The free energy per lattice site expanded up to the fourth order in magnetic moments can then be written as

$$\begin{aligned}
f &= \frac{1}{N^2} \sum_{l,l'}^N \sum_{\alpha,\beta}^{x,y,z} a_{\alpha\beta}(l,l') m_{l\alpha} m_{l'\beta} \\
&+ \frac{1}{N^4} \sum_{l,l',l'',l'''}^N \sum_{\alpha,\beta,\gamma,\delta}^{x,y,z} b_{\alpha\beta\gamma\delta}(l,l',l'',l''') m_{l\alpha} m_{l'\beta} m_{l''\gamma} m_{l'''\delta}.
\end{aligned} \tag{2.1}$$

Here,  $N$  is the number of lattice sites and  $m_{l\alpha}$  denotes the  $\alpha$ -component ( $\alpha = x, y, z$ ) of a magnetic moment on the  $l$ -th site.  $a_{\alpha\beta}(l, l')$  and  $b_{\alpha\beta\gamma\delta}(l, l', l'', l''')$  are the expansion coefficients of the second- and fourth-order terms, respectively.  $\sum_{l,l'}^N (\sum_{l,l',l'',l'''}^N)$  denotes the summations with respect to the site indices  $l$  and  $l'$  ( $l, l', l'',$  and  $l'''$ ) over all integer values from 1 to  $N$ .  $\sum_{\alpha,\beta}^{x,y,z}$  ( $\sum_{\alpha,\beta,\gamma,\delta}^{x,y,z}$ ) denotes the summations with respect to the component indices  $\alpha$  and  $\beta$  ( $\alpha, \beta, \gamma,$  and  $\delta$ ) over  $x, y,$  and  $z$ .

Note that free energy (2.1) is written in the most general way in which each pair (quartet) of local magnetic moments at different sites is coupled via a coefficient independent of those for other pairs (quartets) of local magnetic moments. Therefore, free energy (2.1) can describe the energy costs when the local magnetic moments change their magnitudes and directions, and hence can describe both the incommensurate and commensurate SDWs in itinerant magnets. The same type of free energy expansion has been applied to the incommensurate SDWs of Cr.<sup>36,37</sup>

In the present paper, we apply free energy (2.1) to various SDW states that can be realized on the fcc transition metals, specifically,  $\gamma$ -Fe. Then the free energy must be invariant with respect to the symmetry operations for the magnetic moments on the fcc lattice: rotation  $\mathbf{m}_{\mathbf{R}_l} \rightarrow \mathcal{R}(\mathbf{m}_{\mathbf{R}_l})$ , inversion  $\mathbf{m}_{\mathbf{R}_l} \rightarrow \mathbf{m}_{-\mathbf{R}_l}$ , and translation  $\mathbf{m}_{\mathbf{R}_l} \rightarrow \mathbf{m}_{\mathbf{R}_l + \mathbf{r}}$ . Here,  $\mathbf{R}_l$  is the position vector of the  $l$ -th site;  $\mathbf{m}_{\mathbf{R}_l} \equiv \mathbf{m}_l$  is the magnetic moment at the  $l$ -th site.  $\mathcal{R}$  denotes either the rotation  $C_4[100]$  or  $C_3[111]$ , and  $\mathbf{r}$  denotes an arbitrary lattice translation vector of the fcc lattice. The requirement that the free energy be invariant under these operations yields the following free energy (see Appendix A):

$$\begin{aligned}
f &= \frac{1}{N^2} \sum_{l,l'} A(l,l') \mathbf{m}_l \cdot \mathbf{m}_{l'} \\
&+ \frac{1}{N^4} \sum_{l,l',l'',l'''} [B(l,l',l'',l''') \{ \mathbf{m}_l \cdot \mathbf{m}_{l'} \} \{ \mathbf{m}_{l''} \cdot \mathbf{m}_{l'''} \} \\
&+ C(l,l',l'',l''') \sum_{(\alpha,\beta)}^{(y,z)(z,x)(x,y)} (m_{l\alpha} m_{l'\alpha} m_{l''\beta} m_{l'''\beta} \\
&\quad + m_{l\beta} m_{l'\beta} m_{l''\alpha} m_{l'''\alpha})]. \tag{2.2}
\end{aligned}$$

Here,  $A(l, l') \equiv a_{xx}(l, l')$ ,  $B(l, l', l'', l''') \equiv b_{xxxx}(l, l', l'', l''')$ , and  $C(l, l', l'', l''') \equiv b_{yyzz}(l, l', l'', l''') + b_{yzyz}(l, l', l'', l''') + b_{yyzy}(l, l', l'', l''') - b_{xxxx}(l, l', l'', l''')$ . The second-order terms with  $A(l, l')$  and the fourth-order terms with  $B(l, l', l'', l''')$  in the free energy are isotropic since they are expressed in terms of the

scalar products of magnetic moments. On the other hand, the fourth-order terms with the coefficients  $C(l, l', l'', l''')$  are anisotropic. In the present paper, we restrict ourselves to the transition metals where the spin-orbit coupling effects are negligibly small, and thus neglect the anisotropic terms, i.e., we consider the case  $C(l, l', l'', l''') = 0$  in free energy (2.2).

We now define the Fourier representation of the magnetic moment at  $\mathbf{R}_l$  by

$$\mathbf{m}_l = \sum_{\mathbf{q}}^{\text{EBZ}} \mathbf{m}(\mathbf{q}) e^{i\mathbf{q} \cdot \mathbf{R}_l}, \tag{2.3}$$

where  $\sum_{\mathbf{q}}^{\text{EBZ}}$  denotes a summation with respect to  $\mathbf{q}$  over the extended first Brillouin zone (EBZ) of the fcc lattice, which is defined to include all the zone boundary points. This form, with the use of the EBZ, has the merit that one can argue the structures in both the commensurate and incommensurate cases on the same footing.

The Fourier representation of the isotropic free energy is then given by

$$\begin{aligned}
f &= \sum_{\mathbf{q}}^{\text{EBZ}} A(\mathbf{q}) |\mathbf{m}(\mathbf{q})|^2 + \sum_{\mathbf{K}} \sum_{\mathbf{q}, \mathbf{q}', \mathbf{q}'', \mathbf{q}'''} B(\mathbf{q}, \mathbf{q}', \mathbf{q}'', \mathbf{q}''') \\
&\quad \times \{ \mathbf{m}(\mathbf{q}) \cdot \mathbf{m}(\mathbf{q}') \} \{ \mathbf{m}(\mathbf{q}'') \cdot \mathbf{m}(\mathbf{q}''') \}, \tag{2.4}
\end{aligned}$$

where the coefficients  $A(\mathbf{q})$  and  $B(\mathbf{q}, \mathbf{q}', \mathbf{q}'', \mathbf{q}''')$  are defined by

$$A(\mathbf{q}) = \frac{1}{N} \sum_n A(n) e^{i\mathbf{q} \cdot \mathbf{R}_n}, \tag{2.5}$$

$$\begin{aligned}
B(\mathbf{q}, \mathbf{q}', \mathbf{q}'', \mathbf{q}''') &= \frac{1}{N^3} \sum_{n, n', n''} B(n, n', n'') \\
&\quad \times e^{i\mathbf{q}' \cdot \mathbf{R}_n} e^{i\mathbf{q}'' \cdot \mathbf{R}_{n'}} e^{i\mathbf{q}''' \cdot \mathbf{R}_{n''}} \delta_{\mathbf{q} + \mathbf{q}' + \mathbf{q}'' + \mathbf{q}''', \mathbf{K}}. \tag{2.6}
\end{aligned}$$

In defining the coefficients  $A(\mathbf{q})$  and  $B(\mathbf{q}, \mathbf{q}', \mathbf{q}'', \mathbf{q}''')$  in eqs. (2.5) and (2.6), we have introduced the relative coordinates  $\mathbf{R}_n \equiv \mathbf{R}_l - \mathbf{R}_l$ ,  $\mathbf{R}_{n'} \equiv \mathbf{R}_{l'} - \mathbf{R}_l$ , and  $\mathbf{R}_{n''} \equiv \mathbf{R}_{l''} - \mathbf{R}_l$ , and have used the notations

$$A(n) \equiv A(l, l') = A(\mathbf{R}_l, \mathbf{R}_{l'}) = A(0, \mathbf{R}_n), \tag{2.7}$$

$$\begin{aligned}
B(n, n', n'') &\equiv B(l, l', l'', l''') = B(\mathbf{R}_l, \mathbf{R}_{l'}, \mathbf{R}_{l''}, \mathbf{R}_{l'''}) \\
&= B(0, \mathbf{R}_n, \mathbf{R}_{n'}, \mathbf{R}_{n''}). \tag{2.8}
\end{aligned}$$

Here, the last equalities in eqs. (2.7) and (2.8) result from the translational symmetry of the fcc lattice. Note that the inclusion of the fourth-order terms in free energy (2.1), and hence in eq. (2.4), is essential for the present analysis since the second-order terms alone do not describe the MSDW states.

As is always the case with all Landau-type theories, one should keep in mind the applicability of free energy expansion (2.4), which is valid for the system with small local magnetic moments. In the present paper, our main

concern is the complex magnetic structures of  $\gamma$ -Fe which appear between the nonmagnetic state and the strong ferromagnetic state with increasing volume. In such a region, the magnitudes of the magnetic moments are relatively small. Even if this were not the case, we can apply the theory at any volume near the transition temperature where the local magnetic moments become small. Because of these reasons, we apply free energy expansion (2.4) for the analysis of various SDW states in  $\gamma$ -Fe, i.e., the commensurate  $1\hat{Q}$ ,  $2\hat{Q}$ , and  $3\hat{Q}$  SDWs, and the incommensurate linearly and helically polarized SDWs with  $1Q$ ,  $2Q$ , and  $3Q$  wave vectors. On the basis of the analysis, one can draw a general and exact conclusion independent of the specific model or the potential in the first-principles calculations.

### 3. Commensurate SDW Structures

We investigate here the commensurate SDW structures whose magnetic moments are given by

$$\mathbf{m}_l = \sum_{n=1}^3 [\mathbf{m}(\hat{Q}_n) e^{i\hat{Q}_n \cdot \mathbf{R}_l} + \bar{\mathbf{m}}(\hat{Q}_n) e^{-i\hat{Q}_n \cdot \mathbf{R}_l}], \quad (3.9)$$

with the set of equivalent wave vectors  $\hat{Q}_1 = (1, 0, 0)(2\pi/a)$ ,  $\hat{Q}_2 = (0, 1, 0)(2\pi/a)$ , and  $\hat{Q}_3 = (0, 0, 1)(2\pi/a)$ . Here,  $\mathbf{m}(\hat{Q}_1)$ ,  $\mathbf{m}(\hat{Q}_2)$ , and  $\mathbf{m}(\hat{Q}_3)$  are real and assumed to be orthogonal to each other:  $\mathbf{m}(\hat{Q}_2) \cdot \mathbf{m}(\hat{Q}_3) = \mathbf{m}(\hat{Q}_3) \cdot \mathbf{m}(\hat{Q}_1) = \mathbf{m}(\hat{Q}_1) \cdot \mathbf{m}(\hat{Q}_2) = 0$ . The commensurate MSDW with the form of eq. (3.9) has been discussed in the previous ground-state electronic-structure calculations.<sup>27–29,33</sup> The free energy is given by

$$f_{\text{co}} = \sum_{i=1}^3 [\tilde{A}_Q |\mathbf{m}(\hat{Q}_i)|^2 + (B_{1Q} + \tilde{B}_{2Q}) |\mathbf{m}(\hat{Q}_i)|^4] + \sum_{(i,j)}^{(2,3)(3,1)(1,2)} \tilde{B}_{1QQ} |\mathbf{m}(\hat{Q}_i)|^2 |\mathbf{m}(\hat{Q}_j)|^2. \quad (3.10)$$

The coefficients  $\tilde{A}_Q$ ,  $B_{1Q}$ ,  $\tilde{B}_{2Q}$ , and  $\tilde{B}_{1QQ}$  are expressed in terms of linear combinations of the coefficients  $\{A(\mathbf{q})\}$  and  $\{B(\mathbf{q}, \mathbf{q}', \mathbf{q}'', \mathbf{q}''')\}$  in eqs. (2.5) and (2.6), with  $\mathbf{q}$ ,  $\mathbf{q}'$ ,  $\mathbf{q}''$ , and  $\mathbf{q}'''$  being chosen from  $\pm\hat{Q}_1$ ,  $\pm\hat{Q}_2$ , and  $\pm\hat{Q}_3$ . The full expressions of these coefficients are given in Appendix B. We see that free energy (3.10) depends only on the absolute squares of magnetic moments  $|\mathbf{m}(\hat{Q}_i)|^2$  ( $i = 1, 2, 3$ ). Thus the SDW structures described by this free energy are degenerate with respect to the directions of polarization. This degeneracy is partially removed when the anisotropic terms are included in the free energy. In the following, we investigate three commensurate magnetic structures, the first-kind AF structure, the  $2\hat{Q}$  structure, and the  $3\hat{Q}$  structure, on the basis of free energy (3.10).

#### 3.1 First-kind antiferromagnetic structure

The equilibrium magnetic moment for the first-kind AF structure is obtained by minimizing free energy (3.10) with respect to  $|\mathbf{m}(\hat{Q}_1)|^2$  and setting  $\mathbf{m}(\hat{Q}_2) =$

$\mathbf{m}(\hat{Q}_3) = 0$ . We have

$$|\mathbf{m}(\hat{Q}_1)| = \left[ -\frac{\tilde{A}_Q}{2(B_{1Q} + \tilde{B}_{2Q})} \right]^{1/2}, \quad (3.11)$$

under the condition

$$-\frac{\tilde{A}_Q}{2(B_{1Q} + \tilde{B}_{2Q})} > 0. \quad (3.12)$$

In order for the solution (3.11) to be thermodynamically stable, it is necessary that

$$\left. \frac{\partial^2 f}{\partial \{|\mathbf{m}(\hat{Q}_1)|^2\}^2} \right|_{(3.11)} > 0. \quad (3.13)$$

Inequalities (3.12) and (3.13) reduce to

$$\tilde{A}_Q < 0, \quad (3.14)$$

$$B_{1Q} + \tilde{B}_{2Q} > 0. \quad (3.15)$$

Inequalities (3.14) and (3.15) yield the stability conditions for the first-kind AF structure.

The equilibrium free energy is obtained by substituting eq. (3.11) and  $\mathbf{m}(\hat{Q}_2) = \mathbf{m}(\hat{Q}_3) = 0$  into eq. (3.10):

$$f_{\text{AF}} = -\frac{\tilde{A}_Q^2}{4(B_{1Q} + \tilde{B}_{2Q})}. \quad (3.16)$$

The amplitude  $M$  of the magnetic moment per site is given by

$$M^2 \equiv \frac{1}{N} \sum_l \mathbf{m}_l \cdot \mathbf{m}_l = \sum_{\mathbf{q}, \mathbf{q}'}^{\text{EBZ}} \mathbf{m}(\mathbf{q}) \cdot \mathbf{m}(\mathbf{q}') \sum_{\mathbf{K}} \delta_{\mathbf{q}+\mathbf{q}', \mathbf{K}}. \quad (3.17)$$

In the commensurate case, it becomes

$$M^2 = 4(|\mathbf{m}(\hat{Q}_1)|^2 + |\mathbf{m}(\hat{Q}_2)|^2 + |\mathbf{m}(\hat{Q}_3)|^2). \quad (3.18)$$

Substituting eq. (3.11) and  $\mathbf{m}(\hat{Q}_2) = \mathbf{m}(\hat{Q}_3) = 0$  into eq. (3.18), we have the amplitude  $M_{\text{AF}}$  of the magnetic moment for the first-kind AF structure:

$$M_{\text{AF}}^2 = -\frac{2\tilde{A}_Q}{B_{1Q} + \tilde{B}_{2Q}}. \quad (3.19)$$

#### 3.2 $2\hat{Q}$ structure

The equilibrium magnetic moments for the  $2\hat{Q}$  structure are obtained by minimizing free energy (3.10) with respect to  $|\mathbf{m}(\hat{Q}_1)|^2$  and  $|\mathbf{m}(\hat{Q}_2)|^2$  and setting  $\mathbf{m}(\hat{Q}_3) = 0$ , we have

$$\tilde{A}_Q + 2(B_{1Q} + \tilde{B}_{2Q})|\mathbf{m}(\hat{Q}_1)|^2 + \tilde{B}_{1QQ}|\mathbf{m}(\hat{Q}_2)|^2 = 0, \quad (3.20)$$

$$\tilde{A}_Q + 2(B_{1Q} + \tilde{B}_{2Q})|\mathbf{m}(\hat{Q}_2)|^2 + \tilde{B}_{1QQ}|\mathbf{m}(\hat{Q}_1)|^2 = 0. \quad (3.21)$$

When

$$D_{2\hat{Q}} \equiv 4(B_{1Q} + \tilde{B}_{2Q})^2 - \tilde{B}_{1QQ}^2 \neq 0, \quad (3.22)$$

eqs. (3.20) and (3.21) are solved as

$$|\mathbf{m}(\hat{Q}_1)| = |\mathbf{m}(\hat{Q}_2)| = \left[ -\frac{\tilde{A}_Q}{2(B_{1Q} + \tilde{B}_{2Q}) + \tilde{B}_{1QQ}} \right]^{1/2}, \quad (3.23)$$

under the condition

$$-\frac{\tilde{A}_Q}{2(B_{1Q} + \tilde{B}_{2Q}) + \tilde{B}_{1QQ}} > 0. \quad (3.24)$$

In order for the solution (3.23) to be thermodynamically stable, it is necessary that

$$\delta^2 f = \sum_{i=1}^2 \sum_{j=1}^2 \frac{\partial^2 f}{\partial \{|\mathbf{m}(\hat{Q}_i)|^2\} \partial \{|\mathbf{m}(\hat{Q}_j)|^2\}} \Bigg|_{(3.23)} \times \delta |\mathbf{m}(\hat{Q}_i)|^2 \delta |\mathbf{m}(\hat{Q}_j)|^2 > 0. \quad (3.25)$$

This condition is equivalent to

$$f_{11} > 0, \quad \left| \begin{array}{cc} f_{11} & f_{12} \\ f_{21} & f_{22} \end{array} \right| > 0, \quad (3.26)$$

where  $f_{ij}$  is defined by

$$f_{ij} \equiv \frac{\partial^2 f}{\partial \{|\mathbf{m}(\hat{Q}_i)|^2\} \partial \{|\mathbf{m}(\hat{Q}_j)|^2\}} \Bigg|_{(3.23)} \quad (i, j = 1, 2). \quad (3.27)$$

Using eq. (3.27), condition (3.26) becomes

$$2(B_{1Q} + \tilde{B}_{2Q}) > 0, \quad (3.28)$$

$$4(B_{1Q} + \tilde{B}_{2Q})^2 - \tilde{B}_{1QQ}^2 > 0. \quad (3.29)$$

Conditions (3.22), (3.24), (3.28), and (3.29) reduce to

$$\tilde{A}_Q < 0, \quad (3.30)$$

$$B_{1Q} + \tilde{B}_{2Q} > \frac{|\tilde{B}_{1QQ}|}{2}. \quad (3.31)$$

Inequalities (3.30) and (3.31) yield the stability condition for the  $2\hat{Q}$  structure.

The equilibrium free energy is obtained by substituting eq. (3.23) and  $\mathbf{m}(\hat{Q}_3) = 0$  into eq. (3.10):

$$f_{2\hat{Q}} = -\frac{\tilde{A}_Q^2}{2(B_{1Q} + \tilde{B}_{2Q}) + \tilde{B}_{1QQ}}. \quad (3.32)$$

The amplitude  $M_{2\hat{Q}}$  of the magnetic moment per site is obtained by substituting eq. (3.23) into eq. (3.18):

$$M_{2\hat{Q}}^2 = -\frac{8\tilde{A}_Q}{2(B_{1Q} + \tilde{B}_{2Q}) + \tilde{B}_{1QQ}}. \quad (3.33)$$

### 3.3 $3\hat{Q}$ structure

The equilibrium magnetic moments for the  $3\hat{Q}$  structure are obtained by minimizing free energy (3.10) with respect to  $|\mathbf{m}(\hat{Q}_1)|^2$ ,  $|\mathbf{m}(\hat{Q}_2)|^2$ , and  $|\mathbf{m}(\hat{Q}_3)|^2$ . We obtain

$$|\mathbf{m}(\hat{Q}_1)| = |\mathbf{m}(\hat{Q}_2)| = |\mathbf{m}(\hat{Q}_3)| = \left[ -\frac{\tilde{A}_Q}{2(B_{1Q} + \tilde{B}_{2Q} + \tilde{B}_{1QQ})} \right]^{1/2}, \quad (3.34)$$

under the condition

$$-\frac{\tilde{A}_Q}{2(B_{1Q} + \tilde{B}_{2Q} + \tilde{B}_{1QQ})} > 0. \quad (3.35)$$

The thermodynamical stability analysis and inequality (3.35) lead to the stability condition for the  $3\hat{Q}$  structure:

$$\tilde{A}_Q < 0, \quad (3.36)$$

$$B_{1Q} + \tilde{B}_{2Q} > \frac{\tilde{B}_{1QQ}}{2} \quad \text{for } \tilde{B}_{1QQ} > 0, \quad (3.37)$$

$$B_{1Q} + \tilde{B}_{2Q} > -\tilde{B}_{1QQ} \quad \text{for } \tilde{B}_{1QQ} < 0. \quad (3.38)$$

The equilibrium free energy is obtained by substituting eq. (3.34) into eq. (3.10):

$$f_{3\hat{Q}} = -\frac{3\tilde{A}_Q^2}{4(B_{1Q} + \tilde{B}_{2Q} + \tilde{B}_{1QQ})}. \quad (3.39)$$

The amplitude  $M_{3\hat{Q}}$  of the magnetic moment for the  $3\hat{Q}$  structure is obtained by substituting eq. (3.34) into eq. (3.18):

$$M_{3\hat{Q}}^2 = -\frac{6\tilde{A}_Q}{B_{1Q} + \tilde{B}_{2Q} + \tilde{B}_{1QQ}}. \quad (3.40)$$

### 3.4 Relative stability among commensurate structures

The relative stability among the first-kind AF, and the  $2\hat{Q}$  and  $3\hat{Q}$  structures has been determined by comparing stability conditions (3.14), (3.15), (3.30), (3.31), and (3.36)-(3.38), and equilibrium free energies (3.16), (3.32), and (3.39). The obtained magnetic phase diagram<sup>39</sup> for  $\tilde{A}_Q < 0$  is shown in Fig. 1 in the space of expansion coefficients  $\tilde{B}_{1QQ}/B_{1Q}$  and  $\tilde{B}_{2Q}/B_{1Q}$ , where  $B_{1Q} > 0$  for  $\tilde{B}_{2Q}/B_{1Q} > -1$  and  $B_{1Q} < 0$  for  $\tilde{B}_{2Q}/B_{1Q} < -1$ .

All three commensurate structures appear in the magnetic phase diagram. In the AF phase ( $0 < B_{1Q} + \tilde{B}_{2Q} < |\tilde{B}_{1QQ}|/2$ ), the AF state is the only stable structure. In the  $2\hat{Q}$  phase ( $0 < -\tilde{B}_{1QQ}/2 < B_{1Q} + \tilde{B}_{2Q} < -\tilde{B}_{1QQ}$ ), the AF and  $2\hat{Q}$  structures are stable. Comparison of their free energies shows that the  $2\hat{Q}$  structure is the most stable state in this region. Note that the amplitude of the magnetic moment for the  $2\hat{Q}$  structure is larger than that for the AF structure in this region. In the  $3\hat{Q}$  phase ( $0 < \tilde{B}_{1QQ}/2 < B_{1Q} + \tilde{B}_{2Q}$ ,  $0 < -\tilde{B}_{1QQ} < B_{1Q} + \tilde{B}_{2Q}$ ), all three commensurate structures are stable. Since the equilibrium free energies satisfy the inequality  $f_{AF} > f_{2\hat{Q}} > f_{3\hat{Q}}$ , the  $3\hat{Q}$  structure is the most stable state in this region. The relation among the amplitudes of the magnetic moments for the three structures  $M_{AF} < M_{2\hat{Q}} < M_{3\hat{Q}}$  shows that the  $3\hat{Q}$  structure is the state with the largest magnetic moment in this region.

It is of interest here to compare the present magnetic phase diagram for the commensurate structures with

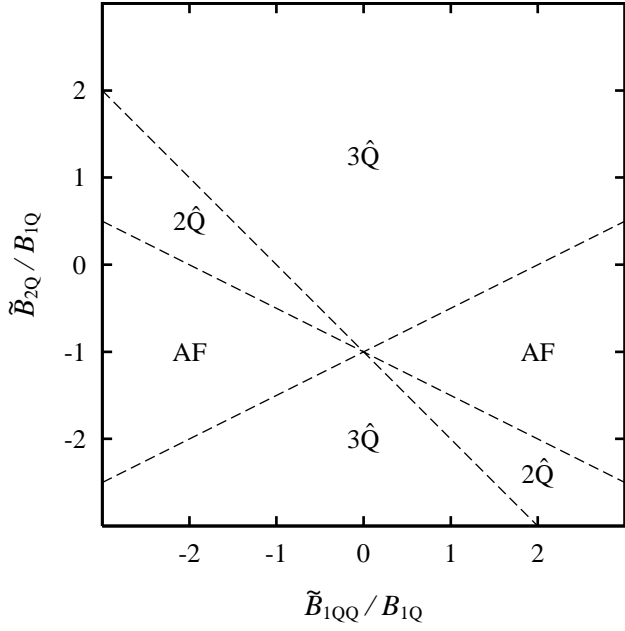


Fig. 1. Magnetic phase diagram for the commensurate structures with  $\hat{Q} = 2\pi/a$  for  $\hat{A}_Q < 0$ . The first-kind antiferromagnetic (AF), and the  $2\hat{Q}$ , and  $3\hat{Q}$  phases are shown in the space of expansion coefficients  $\tilde{B}_{1Q}/B_{1Q}$  and  $\tilde{B}_{2Q}/B_{1Q}$ , where  $B_{1Q} > 0$  for  $\tilde{B}_{2Q}/B_{1Q} > -1$  and  $B_{1Q} < 0$  for  $\tilde{B}_{2Q}/B_{1Q} < -1$ .

the past results of the ground-state electronic-structure calculations for cubic  $\gamma$ -Fe. Those calculations<sup>20–27,32,33</sup> showed that the magnetism of  $\gamma$ -Fe depends sensitively on the volume; the first-kind AF state appears for lattice constants  $a \lesssim 6.5$  a.u., complex magnetic structures for lattice constants  $6.5 \lesssim a \lesssim 7.0$  a.u., and the ferromagnetic state for  $7.0 \lesssim a$ . Although there is a wide diversity in the results of the predicted magnetic structures for intermediate values of the lattice constant,  $6.5 \lesssim a \lesssim 7.0$  a.u., it is worth noting that the ground-state electronic-structure calculations by Kakehashi *et al.*<sup>33</sup> and those by Fujii *et al.*<sup>28</sup> predicted the commensurate  $3\hat{Q}$  state to appear for lattice constants  $a \leq 6.8$  a.u. Kakehashi *et al.*<sup>33</sup> performed the first-principles tight-binding LMTO calculations for  $\gamma$ -Fe using the GGA potential and compared the ground-state energies of various MSDW states. It was predicted that with increasing volume,  $\gamma$ -Fe undergoes a transition from the first-kind AF state to the commensurate  $3\hat{Q}$  state at  $a = 6.5$  a.u. with the  $3\hat{Q}$  state remaining stable until  $a = 6.8$  a.u. This result is consistent with the present magnetic phase diagram of Fig. 1 which shows the possibility of the transition from the AF to the  $3\hat{Q}$  phase crossing the boundary.

Fujii and co-workers<sup>28</sup> found three possible ground states for  $\gamma$ -Fe: the first-kind AF, and the  $2\hat{Q}$  and  $3\hat{Q}$  structures, using the LMTO method and the von Barth-Hedin potential, and found numerically that the  $3\hat{Q}$  structure is the most stable among the three at  $a = 6.8$  a.u. As we mentioned above, the present theory yields the same relative stability,  $f_{AF} > f_{2\hat{Q}} > f_{3\hat{Q}}$ , among the AF,  $2\hat{Q}$ , and  $3\hat{Q}$  structures; their results are verified by the present theory. It is of interest to note that the amplitudes of their magnetic moments for the  $3\hat{Q}$

and  $2\hat{Q}$  structures were found to be the same and larger than that for the AF structure:  $M_{3\hat{Q}} = M_{2\hat{Q}} > M_{AF}$ . According to eqs. (3.33) and (3.40), this implies that  $B_{1Q} + \tilde{B}_{2Q} = \tilde{B}_{1QQ}/2$ ; the ground state of  $\gamma$ -Fe calculated by Fujii *et al.* is located in the vicinity of the AF- $3\hat{Q}$  boundary in the  $3\hat{Q}$  phase in Fig. 1.

#### 4. Incommensurate SDW Structures

We consider SDW structures described by three incommensurate wave vectors  $\mathbf{Q}_1$ ,  $\mathbf{Q}_2$ , and  $\mathbf{Q}_3$ . These wave vectors are assumed to be equivalent in space with each other and to satisfy the following incommensurate conditions:

$$\pm 4\mathbf{Q}_i \neq \mathbf{K}, \quad \pm 2\mathbf{Q}_i \neq \mathbf{K} \quad (i = 1, 2, 3), \quad (4.41)$$

$$\pm 2(\mathbf{Q}_i \pm \mathbf{Q}_j) \neq \mathbf{K}, \quad \pm(3\mathbf{Q}_i \pm \mathbf{Q}_j) \neq \mathbf{K},$$

$$\pm(\mathbf{Q}_i \pm \mathbf{Q}_j) \neq \mathbf{K} \quad ((i, j) = (2, 3)(3, 1)(1, 2)), \quad (4.42)$$

$$\pm(2\mathbf{Q}_i \pm \mathbf{Q}_j \pm \mathbf{Q}_k) \neq \mathbf{K}$$

$$((i, j, k) = (1, 2, 3)(2, 3, 1)(3, 1, 2)). \quad (4.43)$$

Here,  $\mathbf{K}$  is a reciprocal lattice vector of the fcc lattice. Incommensurate conditions (4.41)-(4.43) are satisfied by the wave vectors predicted for the bulk cubic  $\gamma$ -Fe in the electronic band-structure calculations<sup>20,21</sup> and in the molecular-dynamics calculations,<sup>32,33</sup> and by that found in the neutron diffraction measurements<sup>5</sup> of the cubic  $\gamma$ -Fe<sub>100-x</sub>Co<sub>x</sub> ( $x < 4$ ) precipitates in Cu. The free energy describing the incommensurate SDWs can be written as

$$\begin{aligned} f_{ic} = & \sum_{i=1}^3 [A_Q |\mathbf{m}(\mathbf{Q}_i)|^2 + B_{1Q} |\mathbf{m}(\mathbf{Q}_i)|^4 \\ & + B_{2Q} \mathbf{m}^2(\mathbf{Q}_i) \mathbf{m}^{*2}(\mathbf{Q}_i)] \\ & + \sum_{(i,j)}^{(2,3)(3,1)(1,2)} [B_{1QQ} |\mathbf{m}(\mathbf{Q}_i)|^2 |\mathbf{m}(\mathbf{Q}_j)|^2 \\ & + B_{2QQ} |\mathbf{m}(\mathbf{Q}_i) \cdot \mathbf{m}(\mathbf{Q}_j)|^2 + B_{3QQ} |\mathbf{m}(\mathbf{Q}_i) \cdot \mathbf{m}^*(\mathbf{Q}_j)|^2]. \end{aligned} \quad (4.44)$$

The coefficients  $A_Q$ ,  $B_{1Q}$ ,  $B_{2Q}$ ,  $B_{1QQ}$ ,  $B_{2QQ}$ , and  $B_{3QQ}$  are expressed in terms of linear combinations of coefficients  $A(\mathbf{q})$  and  $B(\mathbf{q}, \mathbf{q}', \mathbf{q}'', \mathbf{q}''')$  in eqs. (2.5) and (2.6), with  $\mathbf{q}$ ,  $\mathbf{q}'$ ,  $\mathbf{q}''$ , and  $\mathbf{q}'''$  being chosen from  $\mathbf{Q}_1$ ,  $\mathbf{Q}_2$ , and  $\mathbf{Q}_3$  satisfying conditions (4.41)-(4.43). The full expressions of these coefficients are given in Appendix B. On the basis of free energy (4.44), we investigate the  $1\hat{Q}$ ,  $2\hat{Q}$ , and  $3\hat{Q}$  linearly polarized SDWs, and the  $1\hat{Q}$ ,  $2\hat{Q}$ , and  $3\hat{Q}$  helically polarized SDWs.

##### 4.1 Linearly polarized SDWs

We consider first the linearly polarized SDWs whose magnetic moments are described by

$$\mathbf{m}_l = \sum_{n=1}^3 [\mathbf{m}(\mathbf{Q}_n) e^{i\mathbf{Q}_n \cdot \mathbf{R}_l} + \mathbf{m}^*(\mathbf{Q}_n) e^{-i\mathbf{Q}_n \cdot \mathbf{R}_l}], \quad (4.45)$$

with

$$\mathbf{m}(\mathbf{Q}_n) = (m_x(\mathbf{Q}_n), m_y(\mathbf{Q}_n), m_z(\mathbf{Q}_n))e^{i\alpha_n} \quad (n = 1, 2, 3). \quad (4.46)$$

Here,  $m_x(\mathbf{Q}_n)$ ,  $m_y(\mathbf{Q}_n)$ , and  $m_z(\mathbf{Q}_n)$  ( $n = 1, 2, 3$ ) are assumed to be real.  $\alpha_1$ ,  $\alpha_2$ , and  $\alpha_3$  are phase factors. We consider the case in which  $\mathbf{m}(\mathbf{Q}_1)$ ,  $\mathbf{m}(\mathbf{Q}_2)$ , and  $\mathbf{m}(\mathbf{Q}_3)$  are orthogonal to each other:

$$\mathbf{m}(\mathbf{Q}_2) \cdot \mathbf{m}(\mathbf{Q}_3) = \mathbf{m}(\mathbf{Q}_3) \cdot \mathbf{m}(\mathbf{Q}_1) = \mathbf{m}(\mathbf{Q}_1) \cdot \mathbf{m}(\mathbf{Q}_2) = 0. \quad (4.47)$$

The free energy for the linear SDWs is obtained by substituting eqs. (4.46) and (4.47) into eq. (4.44):

$$f_L = \sum_{i=1}^3 [A_Q |\mathbf{m}(\mathbf{Q}_i)|^2 + (B_{1Q} + B_{2Q}) |\mathbf{m}(\mathbf{Q}_i)|^4] + \sum_{(i,j)}^{(2,3)(3,1)(1,2)} B_{1QQ} |\mathbf{m}(\mathbf{Q}_i)|^2 |\mathbf{m}(\mathbf{Q}_j)|^2. \quad (4.48)$$

Note that free energy (4.48) depends only on the absolute squares of magnetic moments,  $|\mathbf{m}(\mathbf{Q}_1)|^2$ ,  $|\mathbf{m}(\mathbf{Q}_2)|^2$ , and  $|\mathbf{m}(\mathbf{Q}_3)|^2$ . This again implies that the  $1\mathbf{Q}$ ,  $2\mathbf{Q}$ , and  $3\mathbf{Q}$  states are degenerate with respect to the directions of polarization. This degeneracy is partially removed when the anisotropic terms are included in the free energy. We also note that free energy (4.48) has the same form as eq. (3.10) in which  $\tilde{A}_Q$ ,  $\tilde{B}_{2Q}$ , and  $\tilde{B}_{1QQ}$  have been replaced by  $A_Q$ ,  $B_{2Q}$ , and  $B_{1QQ}$ , respectively. Therefore, following the same steps as in §3, we obtain the equilibrium states of the  $1\mathbf{Q}$ ,  $2\mathbf{Q}$ , and  $3\mathbf{Q}$  linear SDWs as follows.

#### 4.1.1 $1\mathbf{Q}$ linearly polarized SDW

Magnetic moment

$$|\mathbf{m}(\mathbf{Q}_1)| = \left[ -\frac{A_Q}{2(B_{1Q} + B_{2Q})} \right]^{1/2}. \quad (4.49)$$

Stability condition

$$A_Q < 0, \quad (4.50)$$

$$B_{1Q} + B_{2Q} > 0. \quad (4.51)$$

Equilibrium free energy

$$f_{1Q} = -\frac{A_Q^2}{4(B_{1Q} + B_{2Q})}. \quad (4.52)$$

Amplitude of the magnetic moment

$$M_{1Q}^2 = 2|\mathbf{m}(\mathbf{Q}_1)|^2 = -\frac{A_Q}{B_{1Q} + B_{2Q}}. \quad (4.53)$$

#### 4.1.2 $2\mathbf{Q}$ linearly polarized SDW

Magnetic moment

$$|\mathbf{m}(\mathbf{Q}_1)| = |\mathbf{m}(\mathbf{Q}_2)| = \left[ -\frac{A_Q}{2(B_{1Q} + B_{2Q}) + B_{1QQ}} \right]^{1/2}. \quad (4.54)$$

Stability condition

$$A_Q < 0, \quad (4.55)$$

$$B_{1Q} + B_{2Q} > \frac{|B_{1QQ}|}{2}. \quad (4.56)$$

Equilibrium free energy

$$f_{2Q} = -\frac{A_Q^2}{2(B_{1Q} + B_{2Q}) + B_{1QQ}}. \quad (4.57)$$

Amplitude of the magnetic moment

$$M_{2Q}^2 = -\frac{4A_Q}{2(B_{1Q} + B_{2Q}) + B_{1QQ}}. \quad (4.58)$$

#### 4.1.3 $3\mathbf{Q}$ linearly polarized SDW

Magnetic moment

$$|\mathbf{m}(\mathbf{Q}_1)| = |\mathbf{m}(\mathbf{Q}_2)| = |\mathbf{m}(\mathbf{Q}_3)| = \left[ -\frac{A_Q}{2(B_{1Q} + B_{2Q} + B_{1QQ})} \right]^{1/2}. \quad (4.59)$$

Stability condition

$$A_Q < 0, \quad (4.60)$$

$$B_{1Q} + B_{2Q} > \frac{B_{1QQ}}{2} \quad \text{for } B_{1QQ} > 0, \quad (4.61)$$

$$B_{1Q} + B_{2Q} > -B_{1QQ} \quad \text{for } B_{1QQ} < 0. \quad (4.62)$$

Equilibrium free energy

$$f_{3Q} = -\frac{3A_Q^2}{4(B_{1Q} + B_{2Q} + B_{1QQ})}. \quad (4.63)$$

Amplitude of the magnetic moment

$$M_{3Q}^2 = -\frac{3A_Q}{B_{1Q} + B_{2Q} + B_{1QQ}}. \quad (4.64)$$

#### 4.2 Relative stability among linear SDWs

The relative stability among the incommensurate  $1\mathbf{Q}$ ,  $2\mathbf{Q}$ , and  $3\mathbf{Q}$  linear SDWs has been determined by comparing stability conditions (4.50)-(4.51), (4.55)-(4.56) and (4.60)-(4.62), and equilibrium free energies (4.52), (4.57), and (4.63). The obtained magnetic phase diagram for  $A_Q < 0$  is shown in Fig. 2 in the space of expansion coefficients  $B_{1QQ}/B_{1Q}$  and  $B_{2Q}/B_{1Q}$ , where  $B_{1Q} > 0$  for  $B_{2Q}/B_{1Q} > -1$  and  $B_{1Q} < 0$  for  $B_{2Q}/B_{1Q} < -1$ .

The relative stability among the linear SDWs has been found to have the same feature as that of the relative stability among the commensurate SDWs. In the  $1\mathbf{Q}$  phase ( $0 < B_{1Q} + B_{2Q} < |B_{1QQ}|/2$ ), the  $1\mathbf{Q}$  linear SDW is the only stable structure. In the  $2\mathbf{Q}$  phase ( $0 < -B_{1QQ}/2 < B_{1Q} + B_{2Q} < -B_{1QQ}$ ), both the  $1\mathbf{Q}$  and  $2\mathbf{Q}$  linear SDWs are stable, but the latter has a lower free energy and larger amplitude of the magnetic moment. In the  $3\mathbf{Q}$  phase ( $0 < B_{1QQ}/2 < B_{1Q} + B_{2Q}$ ,  $0 < -B_{1QQ} < B_{1Q} + B_{2Q}$ ), all three linear SDWs are stable, and the  $3\mathbf{Q}$  state has the lowest free energy and the largest amplitude of the magnetic moment.

Concerning the magnetism of  $\gamma$ -Fe, the present magnetic phase diagram for the linear SDWs indicates the possibility of the  $3\mathbf{Q}$  and  $2\mathbf{Q}$  MSDWs as well as the  $1\mathbf{Q}$  SDW. In the ground-state calculations of bulk cubic  $\gamma$ -Fe, although the magnetic structure for lattice constants  $6.5 \lesssim a \lesssim 7.0$  a.u. is under debate, the possibility of incommensurate linear MSDW was sug-

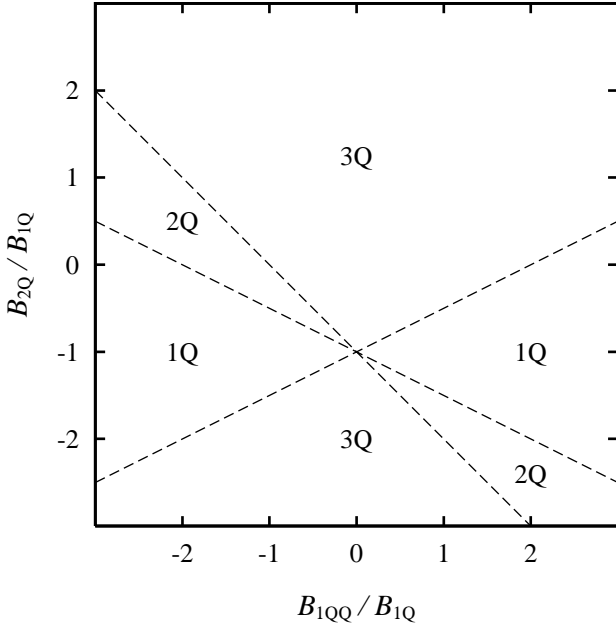


Fig. 2. Magnetic phase diagram for the incommensurate linear SDWs for  $A_Q < 0$ . The  $1\mathbf{Q}$ , the  $2\mathbf{Q}$ , and the  $3\mathbf{Q}$  phase are shown in the space of expansion coefficients  $B_{1QQ}/B_{1Q}$  and  $B_{2Q}/B_{1Q}$ , where  $B_{1Q} > 0$  for  $B_{2Q}/B_{1Q} > -1$  and  $B_{1Q} < 0$  for  $B_{2Q}/B_{1Q} < -1$ .

gested by Kakehashi and coworkers<sup>32,33</sup>. On the basis of the molecular-dynamics (MD) method,<sup>32</sup> they predicted a new MSDW whose principal terms consist of  $3\mathbf{Q}$  waves with  $\mathbf{Q} = (0.6, 0, 0)(2\pi/a)$ ,  $(0, 0.6, 0)(2\pi/a)$ , and  $(0, 0, 0.6)(2\pi/a)$ . Subsequently, they performed the ground-state electronic-structure calculations<sup>33</sup> using the first-principles tight-binding LMTO method and the GGA potentials to compare the ground-state energies of various magnetic structures: the first-kind AF state, the commensurate  $3\mathbf{Q}$  structure, the incommensurate  $1\mathbf{Q}$  helical SDW, the incommensurate MSDW found in the MD calculations, and the ferromagnetic state. It was concluded that the MSDW becomes the most stable state for lattice constants  $6.8 \leq a \leq 7.0$  a.u. In particular, they find that the incommensurate  $3\mathbf{Q}$  MSDW is stable as compared with the  $1\mathbf{Q}$  SDW irrespective of the lattice constant and that the amplitude of the magnetic moment for the  $3\mathbf{Q}$  state is larger than that for the  $1\mathbf{Q}$  state. These results are consistent with the present result that the  $3\mathbf{Q}$  MSDW is always stabilized and has a larger amplitude of the magnetic moment as compared with the  $1\mathbf{Q}$  SDW when the  $3\mathbf{Q}$  solution exists, resulting in a wide range of the  $3\mathbf{Q}$  phase in the magnetic phase diagram in Fig. 2.

#### 4.3 Helically polarized SDWs

Next, we consider the helically polarized SDWs whose magnetic moments are described by

$$\mathbf{m}_l = \sum_{j=1}^3 \sqrt{2} |\mathbf{m}(\mathbf{Q}_j)| [e_k \cos(\mathbf{Q}_j \cdot \mathbf{R}_l + \alpha_j) + e_m \sin(\mathbf{Q}_j \cdot \mathbf{R}_l + \alpha_j)]. \quad (4.65)$$

Here,  $(j, k, m)$  is  $(1, 2, 3)$ ,  $(2, 3, 1)$ , and  $(3, 1, 2)$  when  $j = 1, 2$ , and  $3$ , respectively.  $\mathbf{e}_1$ ,  $\mathbf{e}_2$ , and  $\mathbf{e}_3$  form an orthonormal basis set.  $\alpha_1$ ,  $\alpha_2$ , and  $\alpha_3$  are phase factors. Note that the possibility of the helical  $3\mathbf{Q}$  MSDW given by eq. (4.65) has not been examined in either the experimental analyses or the electronic-structure calculations.

Introducing the basis set  $(\hat{\mathbf{e}}_{jk}, \hat{\mathbf{e}}_{jm})$  obtained by a rotation of  $(\mathbf{e}_k, \mathbf{e}_m)$  by  $\alpha_j$  ( $(j, k, m) = (1, 2, 3)(2, 3, 1)(3, 1, 2)$ ) for each helical component  $j$ ,

$$\hat{\mathbf{e}}_{jk} = \mathbf{e}_k \cos \alpha_j + \mathbf{e}_m \sin \alpha_j, \quad (4.66)$$

$$\hat{\mathbf{e}}_{jm} = -\mathbf{e}_k \sin \alpha_j + \mathbf{e}_m \cos \alpha_j, \quad (4.67)$$

we have the expression

$$\mathbf{m}_l = \sum_{j=1}^3 [\mathbf{m}(\mathbf{Q}_j) e^{i\mathbf{Q}_j \cdot \mathbf{R}_l} + \mathbf{m}^*(\mathbf{Q}_j) e^{-i\mathbf{Q}_j \cdot \mathbf{R}_l}]. \quad (4.68)$$

Here,

$$\mathbf{m}(\mathbf{Q}_j) = \frac{|\mathbf{m}(\mathbf{Q}_j)|}{\sqrt{2}} (\hat{\mathbf{e}}_{jk} - i\hat{\mathbf{e}}_{jm})$$

$$((j, k, m) = (1, 2, 3)(2, 3, 1)(3, 1, 2)). \quad (4.69)$$

The free energy for the helical SDWs is obtained by substituting eq. (4.69) into eq. (4.44):

$$f_H = \sum_{i=1}^3 [A_Q |\mathbf{m}(\mathbf{Q}_i)|^2 + B_{1Q} |\mathbf{m}(\mathbf{Q}_i)|^4] + \sum_{(i,j) = (2,3)(3,1)(1,2)} (B_{1QQ} + B_{2QQH}) |\mathbf{m}(\mathbf{Q}_i)|^2 |\mathbf{m}(\mathbf{Q}_j)|^2, \quad (4.70)$$

with

$$B_{2QQH} \equiv \frac{B_{2QQ} + B_{3QQ}}{4}. \quad (4.71)$$

Note that free energy (4.70) depends only on the absolute squares of magnetic moments  $|\mathbf{m}(\mathbf{Q}_1)|^2$ ,  $|\mathbf{m}(\mathbf{Q}_2)|^2$ , and  $|\mathbf{m}(\mathbf{Q}_3)|^2$ ; therefore, the  $1\mathbf{Q}$ ,  $2\mathbf{Q}$ , and  $3\mathbf{Q}$  helical states are degenerate with respect to the directions of polarization. We also note that free energy (4.70) is identical to eq. (3.10) in which  $\tilde{A}_Q$ ,  $B_{1Q} + \tilde{B}_{2Q}$ , and  $\tilde{B}_{1QQ}$  have been replaced by  $A_Q$ ,  $B_{1Q}$ , and  $B_{1QQ} + B_{2QQH}$ . Thus, following the same steps as in §3, we obtain the equilibrium states of  $1\mathbf{Q}$ ,  $2\mathbf{Q}$ , and  $3\mathbf{Q}$  helical SDWs as follows.

##### 4.3.1 $1\mathbf{Q}$ helically polarized SDW

Magnetic moment

$$|\mathbf{m}(\mathbf{Q}_1)| = \left[ -\frac{A_Q}{2B_{1Q}} \right]^{1/2}. \quad (4.72)$$

Stability condition

$$A_Q < 0, \quad (4.73)$$

$$B_{1Q} > 0. \quad (4.74)$$

Equilibrium free energy



$$f_{1QH} = -\frac{A_Q^2}{4B_{1Q}}. \quad (4.75)$$

Amplitude of the magnetic moment

$$M_{1QH}^2 = -\frac{A_Q}{B_{1Q}}. \quad (4.76)$$

#### 4.3.2 $2Q$ helically polarized SDW

Magnetic moment

$$|\mathbf{m}(\mathbf{Q}_1)| = |\mathbf{m}(\mathbf{Q}_2)| = \left[ -\frac{A_Q}{2B_{1Q} + B_{1QQ} + B_{2QQH}} \right]^{1/2}. \quad (4.77)$$

Stability condition

$$A_Q < 0, \quad (4.78)$$

$$B_{1Q} > \frac{1}{2}|B_{1QQ} + B_{2QQH}|. \quad (4.79)$$

Equilibrium free energy

$$f_{2QH} = -\frac{A_Q^2}{2B_{1Q} + B_{1QQ} + B_{2QQH}}. \quad (4.80)$$

Amplitude of the magnetic moment

$$M_{2QH}^2 = -\frac{4A_Q}{2B_{1Q} + B_{1QQ} + B_{2QQH}}. \quad (4.81)$$

#### 4.3.3 $3Q$ helically polarized SDW

Magnetic moment

$$\begin{aligned} |\mathbf{m}(\mathbf{Q}_1)| &= |\mathbf{m}(\mathbf{Q}_2)| = |\mathbf{m}(\mathbf{Q}_3)| \\ &= \left[ -\frac{A_Q}{2(B_{1Q} + B_{1QQ} + B_{2QQH})} \right]^{1/2}. \end{aligned} \quad (4.82)$$

Stability condition

$$A_Q < 0, \quad (4.83)$$

$$B_{1Q} > \frac{B_{1QQ} + B_{2QQH}}{2} \quad \text{for } B_{1QQ} + B_{2QQH} > 0, \quad (4.84)$$

$$B_{1Q} > -(B_{1QQ} + B_{2QQH}) \quad \text{for } B_{1QQ} + B_{2QQH} < 0. \quad (4.85)$$

Equilibrium free energy

$$f_{3QH} = -\frac{3A_Q^2}{4(B_{1Q} + B_{1QQ} + B_{2QQH})}. \quad (4.86)$$

Amplitude of the magnetic moment

$$M_{3QH}^2 = -\frac{3A_Q}{B_{1Q} + B_{1QQ} + B_{2QQH}}. \quad (4.87)$$

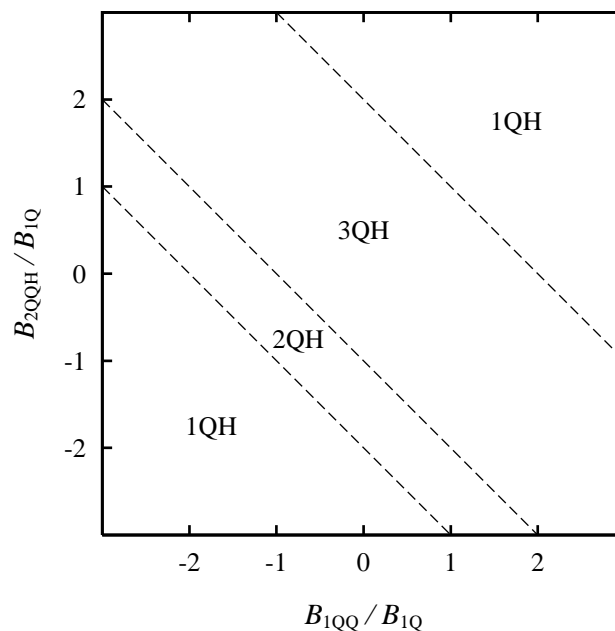


Fig. 3. Magnetic phase diagram for the helical SDWs for  $A_Q < 0$  and  $B_{1Q} > 0$ . The  $1Q$  helical (1QH),  $2Q$  helical (2QH), and  $3Q$  helical (3QH) phases are shown in the space of expansion coefficients  $B_{1QQ}/B_{1Q}$  and  $B_{2QQH}/B_{1Q}$ .

#### 4.4 Relative stability among helical SDWs

The relative stability among the incommensurate  $1Q$ ,  $2Q$ , and  $3Q$  helical SDWs has been determined by comparing stability conditions (4.73)-(4.74), (4.78)-(4.79) and (4.83)-(4.85), and the equilibrium free energies (4.75), (4.80), and (4.86). The obtained magnetic phase diagram is shown in Fig. 3 in the space of expansion coefficients  $B_{1QQ}/B_{1Q}$  and  $B_{2QQH}/B_{1Q}$  for  $A_Q < 0$  and  $B_{1Q} > 0$  for which the solutions of helical SDWs exist.

The relative stability among the helical SDWs has been found to have the same feature as that of the relative stability among the commensurate SDWs and among the linear SDWs. In the  $1Q$  phase ( $0 < B_{1Q} < |B_{1QQ} + B_{2QQH}|/2$ ), the  $1Q$  helical SDW is the only stable structure. In the  $2Q$  phase ( $0 < -(B_{1QQ} + B_{2QQH})/2 < B_{1Q} < -(B_{1QQ} + B_{2QQH})$ ), both the  $1Q$  and  $2Q$  helical SDWs are stable, but the latter has a lower free energy and larger amplitude of the magnetic moment. In the  $3Q$  phase ( $0 < (B_{1QQ} + B_{2QQH})/2 < B_{1Q}$ ,  $0 < -(B_{1QQ} + B_{2QQH}) < B_{1Q}$ ), all the three helical SDWs are stable, but the  $3Q$  state yields the lowest free energy and the largest amplitude of the magnetic moment.

Neutron diffraction experiments<sup>5</sup> on cubic  $\gamma$ -Fe<sub>100-x</sub>Co<sub>x</sub> ( $x < 4$ ) alloy precipitates in Cu showed a magnetic satellite peak for wave vector  $\mathbf{Q} = (0.1, 0, 1)2\pi/a$ . The magnetic structure was suggested to be a helical SDW but has not been determined precisely. This is because the neutron diffraction analysis cannot distinguish between the  $1Q$  and  $3Q$  states<sup>40</sup> when the crystal structure of the  $\gamma$ -Fe precipitates is properly cubic and the distribution of domains is isotropic. The present finding that the  $3Q$  helical MSDW is always stable as compared with the  $1Q$  and

$2Q$  SDWs when the  $3Q$  solution exists suggests that the  $3Q$  helical MSDW should be taken into consideration in addition to the  $1Q$  helical SDW in the analysis of the magnetic structure of cubic  $\gamma$ -Fe.

One might have a question as to why the  $3Q$  MSDW is stable in a wide range of the parameter region (4.84) or (4.85), while the previous phenomenological theories concerning the Heisenberg model<sup>41–43</sup> predict the  $1Q$  helical SDW ground state. The physical reason for this is as follows. For simplicity, we consider first the free energy for the helical SDW states eq. (4.70) without the mode-mode coupling term (the term with  $(B_{1QQ} + B_{2QQH})$ ). The free energy for the  $3Q$  state is three times smaller than that for the  $1Q$  state, as is seen from eqs. (4.75) and (4.86). This free energy gain is caused by the increase in amplitudes of local magnetic moments as is seen from eqs. (4.76) and (4.87). This is characteristic of the itinerant electron system. In the localized model reported by Yoshimori<sup>41</sup> and Kaplan,<sup>42,43</sup> this mechanism of energy gain is forbidden because of the constraint of the constant amplitudes of local magnetic moments, so that the  $1Q$  state is realized. Under the constraint of a constant amplitude of local magnetic moments, the present theory also predicts the  $1Q$  helical SDW as the stable structure, which is consistent with the theory presented by Yoshimori and Kaplan.

When the mode-mode coupling term is positive, it suppresses the increase in the amplitudes of local moments of the  $3Q$  state (see eqs. (4.76) and (4.87)). As a result, the  $3Q$  MSDW is stable only when the coefficient of the mode-mode coupling term is smaller than a critical value; otherwise, the  $1Q$  helical SDW is stable. This condition is given by inequality (4.84).

#### 4.5 Relative stability among linear and helical SDWs

In the previous two subsections, we examined the relative stability among the linear SDWs and that among the helical SDWs, separately, assuming incommensurate conditions (4.41)-(4.43) for the wave vectors. Free energy (4.44) having such incommensurate wave vectors, however, allows for both linear and helical SDWs in the common space of the expansion coefficients. In order to discuss their relative stability, we present, in this subsection, a magnetic phase diagram allowing for both linear and helical SDWs.

Comparing the equilibrium free energies for the linear and helical SDWs, we have obtained magnetic phase diagrams<sup>44</sup> for  $A_Q < 0$  and  $B_{1Q} > 0$  for which both the linear and helical SDWs are stable. Figure 4 shows an example of the magnetic phase diagram for  $B_{2QQH}/B_{1Q} = 1$  in the space of expansion coefficients  $B_{1QQ}/B_{1Q}$  and  $B_{2Q}/B_{1Q}$ , where  $A_Q < 0$  and  $B_{1Q} > 0$ . We see that the  $3Q$  linear ( $3Q$ ) and  $3Q$  helical ( $3QH$ ) MSDWs occupy most of the region  $-2 < B_{1QQ}/B_{1Q} < 1$ . This arises from the fact that the  $3Q$  state is stable when the mode-mode coupling term  $B_{1QQ}$  or  $B_{1QQ} + B_{2QQH}$  is relatively small, as discussed in §4.4. Although we presented an example of the magnetic phase diagram for  $B_{2QQH}/B_{1Q} = 1$  in Fig. 4, changing the value of  $B_{2QQH}/B_{1Q}$  does not alter the global feature of the magnetic phase diagram if it does not become exceedingly large. Thus we discuss the

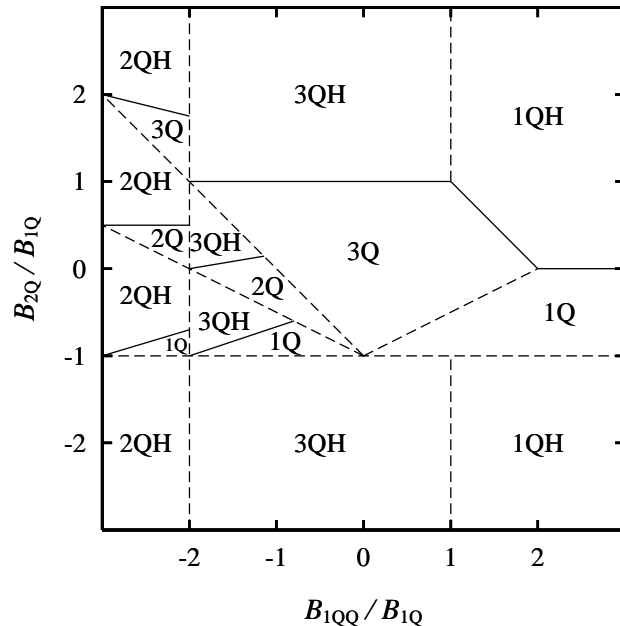


Fig. 4. Magnetic phase diagram for the incommensurate SDWs for  $A_Q < 0$ ,  $B_{1Q} > 0$  and  $B_{2QQH}/B_{1Q} = 1$ . The phases of the  $1Q$  linear SDW ( $1Q$ ), the  $2Q$  linear MSDW ( $2Q$ ), the  $3Q$  linear MSDW ( $3Q$ ), the  $1Q$  helical SDW ( $1QH$ ), the  $2Q$  helical MSDW ( $2QH$ ), and the  $3Q$  helical MSDW ( $3QH$ ) are shown in the space of expansion coefficients  $B_{1QQ}/B_{1Q}$  and  $B_{2Q}/B_{1Q}$ . Coexistence lines between the linear and helical SDWs are indicated by solid lines.

possible magnetic structures of  $\gamma$ -Fe on the basis of the magnetic phase diagram in Fig. 4.

According to the ground-state electronic-structure calculations by Kakehashi *et al.*,<sup>33</sup> the  $3Q$  linear MSDW is stabilized for lattice constants  $6.8 < a < 7.0$  a.u. This result can be explained by the existence of the  $3Q$  linear MSDW phase in Fig. 4. Note that the  $3Q$  linear MSDW solution is extended to the region of the  $3Q$  helical MSDW in Fig. 4. Thus there is another possibility that the latter MSDW is stable when the  $3Q$  helical MSDW is taken into account in the electronic-structure calculations. It is highly desirable to investigate the relative stability between  $3Q$  linear and helical MSDWs in the first-principles ground-state calculations of  $\gamma$ -Fe.

## 5. Summary and Discussion

We have investigated the relative stability among various SDW structures in fcc transition metals on the basis of a Ginzburg-Landau type of free energy with the terms up to the fourth order in magnetic moments. We have obtained magnetic phase diagrams in the space of expansion coefficients for both commensurate and incommensurate wave vectors, and discussed their implications on the magnetism of cubic  $\gamma$ -Fe.

In both the commensurate and incommensurate cases, we proved that the  $3Q$  state is always stable compared with the corresponding  $2Q$  and  $1Q$  states when there is a solution of the  $3Q$  state. The energy gain of the  $3Q$  state is caused by a change in the amplitude of the magnetic moment when an additional mode  $Q$  is introduced. Accordingly, we have the relation  $M_{3Q} > M_{2Q} > M_{1Q}$ . This is characteristic of itinerant magnets and has a profound

effect on the magnetic phase diagram. In the localized systems, only the  $1\mathbf{Q}$  helical SDW is possible because of the fixed amplitudes of local magnetic moments.

On the basis of the magnetic phase diagrams for the commensurate case (Fig. 1) and for the incommensurate case (Figs. 2-4), we have discussed the possible magnetic structures of cubic  $\gamma$ -Fe. According to the ground-state electronic-structure calculations,<sup>20-27, 32, 33</sup> the magnetism of  $\gamma$ -Fe depends sensitively on the volume; the first-kind AF state appears for lattice constants  $a \lesssim 6.5$  a.u., SDW structures for lattice constants  $6.5 \lesssim a \lesssim 7.0$  a.u., and the ferromagnetic state for  $a \gtrsim 7.0$  a.u. The magnetic structures for  $6.5 \lesssim a \lesssim 7.0$  a.u. are under debate and there is a wide diversity in the predicted results.

The ground-state electronic-structure calculations by Takehashi *et al.*<sup>33</sup> and those by Fujii *et al.*<sup>28</sup> predicted the commensurate  $3\hat{\mathbf{Q}}$  state to appear for lattice constants  $a \leq 6.8$  a.u. This result can be explained by the existence of the commensurate  $3\hat{\mathbf{Q}}$  phase, as shown in Fig. 1, specifically in the region of the phase diagram with  $\tilde{B}_{1\mathbf{Q}\mathbf{Q}} \approx 2(B_{1\mathbf{Q}} + \tilde{B}_{2\mathbf{Q}})$  and  $\tilde{B}_{1\mathbf{Q}\mathbf{Q}} > 0$ .

For larger lattice constants,  $6.8 \leq a \leq 7.0$ , the MD calculations<sup>33</sup> for  $\gamma$ -Fe predicted the incommensurate  $3\mathbf{Q}$  linear MSDW state with  $\mathbf{Q} = (0.6, 0, 0)2\pi/a$ ,  $(0, 0.6, 0)2\pi/a$ , and  $(0, 0, 0.6)2\pi/a$ . This can be explained by the existence of the  $3\mathbf{Q}$  linear MSDW phase in Fig. 4. It should be noted, however, that there is another possibility of the  $3\mathbf{Q}$  helical phase since the  $3\mathbf{Q}$  linear MSDW solution is extended to the region of the  $3\mathbf{Q}$  helical phase. It is desirable to examine the relative stability between the  $3\mathbf{Q}$  linear and helical states for the above wave vector by means of the ground-state electronic-structure calculations.

Experimentally, the SDW of cubic  $\gamma$ -Fe was found for wave vector  $\mathbf{Q} = (0.1, 0, 1)2\pi/a$ .<sup>5</sup> It was suggested that a helical spin configuration is a more highly possible structure of the SDW on the basis of the observation that there were no appreciable indications of a strain wave with  $2\mathbf{Q}$  and there was no third-harmonic component. Following that work, most of the ground-state calculations for  $\gamma$ -Fe were concentrated on finding a wave vector which minimizes the energy within the  $1\mathbf{Q}$  helical structure. It should be emphasized, however, that the  $3\mathbf{Q}$  helical MSDW with  $\mathbf{Q} = (0.1, 0, 1)2\pi/a$ ,  $(1, 0.1, 0)2\pi/a$ , and  $(0, 1, 0.1)2\pi/a$  is also consistent with the experimental results. This is because the neutron diffraction analysis cannot distinguish between the  $1\mathbf{Q}$  and  $3\mathbf{Q}$  states<sup>40</sup> when the crystal structure of the  $\gamma$ -Fe precipitates is properly cubic and the distribution of domains is isotropic. The MD approach presented by Takehashi and co-workers<sup>31-33</sup> can predict the ground state without assuming the magnetic structure at the beginning. The resolution for a wave vector of magnetic structure in the MD calculations, however, is  $\delta \geq 0.2$  (in units of  $2\pi/a$ ) at the present stage; therefore it cannot reproduce the MSDW having the observed fraction ( $\delta = 0.1$ ).<sup>5</sup> One needs more accurate ground-state electronic-structure calculations to allow for the possibility of the  $3\mathbf{Q}$  helical MSDW with the experimental wave vector.

Regarding the consistency between theory and experiment, it should also be noted that although the experimentally suggested magnetic structure is a helical SDW,<sup>5</sup> one should not exclude the possibility of the commensurate<sup>28, 33</sup> and linear<sup>33</sup> MSDWs which were found in the ground-state calculations for  $\gamma$ -Fe, because of the strong dependence of the magnetism of  $\gamma$ -Fe on the volume and strain. Experimentally, the SDW of cubic  $\gamma$ -Fe is found in a narrow range of lattice constants approximately equal to that of Cu, and the volume dependence of the magnetic structure of cubic  $\gamma$ -Fe has not been investigated. It is also noted that the possibility of a small lattice distortion is suggested at the onset of the  $1\mathbf{Q}$  SDW in the  $\gamma$ -Fe precipitates in Cu,<sup>45</sup> which might change the stable structure of  $\gamma$ -Fe.

In the present phenomenological analysis, we focussed upon the magnetism of fcc transition metals, specifically, that of cubic  $\gamma$ -Fe. Because the spin-orbit coupling effects are small in these systems, we neglected the anisotropic terms  $C(l, l', l'', l''')$  in free energy (2.2). In order to examine the effect of anisotropy, we also calculated the magnetic phase diagrams including the anisotropic terms in the free energy. We found two main effects. First, inclusion of the anisotropic term partially removes the degeneracy of each SDW state; the most stable states become the SDWs having the longitudinal and transverse polarizations with respect to the  $x$ ,  $y$ , and  $z$  axes, or the superposition of the three longitudinally (transversely) polarized states. Note that the longitudinal and transverse SDWs are still degenerate there relative to each other. Second, the phase boundary between SDW states is subject to a small displacement due to the anisotropy, but the global features of the magnetic phase diagrams in Figs. 1-4 remain qualitatively the same as long as the anisotropic terms are sufficiently small; the conclusions of the present work are not changed by considering the anisotropic terms.

## Acknowledgments

We are grateful to Professor Y. Tsunoda for valuable discussions on the experimental aspects of the SDW states of the cubic  $\gamma$ -Fe precipitates in Cu.

## Appendix A: Derivation of Free Energy (2.2)

In this appendix, we derive the expression of real-space free energy (2.2) using the symmetry argument for the cubic system. We start from free energy expansion (2.1):

$$f = \frac{1}{N^2} \sum_{l, l'}^N \sum_{\alpha, \beta}^{x, y, z} a_{\alpha\beta}(l, l') m_{l\alpha} m_{l'\beta} + \frac{1}{N^4} \sum_{l, l', l'', l'''}^N \sum_{\alpha, \beta, \gamma, \delta}^{x, y, z} b_{\alpha\beta\gamma\delta}(l, l', l'', l''') \times m_{l\alpha} m_{l'\beta} m_{l''\gamma} m_{l'''\delta}. \quad (\text{A}\cdot 1)$$

For the fcc system, free energy (A.1) must be invariant with respect to  $\pi/2$  rotations of magnetic moments about the  $x$ ,  $y$ , and  $z$  axes. It follows that the expansion coefficients satisfy the following relations:

$$a_{\alpha\alpha}(l, l') \text{'s are the same for } \alpha = x, y, z, \quad (\text{A}\cdot 2)$$

$$a_{\alpha\beta}(l, l') = 0 \quad \text{for } \alpha \neq \beta \quad (\alpha, \beta = x, y, z), \quad (\text{A}\cdot 3)$$

$$b_{\alpha\alpha\alpha}(l, l', l'', l''') \text{'s are the same for } \alpha = x, y, z, \quad (\text{A}\cdot 4)$$

$$b_{\text{P}(\alpha\alpha\alpha\beta)}(l, l', l'', l''') = 0 \quad \text{for } \alpha \neq \beta \quad (\alpha, \beta = x, y, z), \quad (\text{A}\cdot 5)$$

$b_{\alpha\alpha\beta\beta}(l, l', l'', l''')$ 's are the same

$$\text{for } (\alpha, \beta) = (y, z)(z, y)(z, x)(x, z)(x, y)(y, x), \quad (\text{A}\cdot 6)$$

$b_{\alpha\beta\beta\alpha}(l, l', l'', l''')$ 's are the same

$$\text{for } (\alpha, \beta) = (y, z)(z, y)(z, x)(x, z)(x, y)(y, x), \quad (\text{A}\cdot 7)$$

$b_{\alpha\beta\alpha\beta}(l, l', l'', l''')$ 's are the same

$$\text{for } (\alpha, \beta) = (y, z)(z, y)(z, x)(x, z)(x, y)(y, x), \quad (\text{A}\cdot 8)$$

$$b_{\text{P}(\alpha\alpha\beta\gamma)}(l, l', l'', l''') = 0$$

$$\text{for } \alpha \neq \beta \neq \gamma \quad (\alpha, \beta, \gamma = x, y, z). \quad (\text{A}\cdot 9)$$

Here, the subscripts P( $\alpha\alpha\beta$ ) in eq. (A.5) and P( $\alpha\alpha\beta\gamma$ ) in eq. (A.9) denote permutation of indices in the parentheses. By virtue of the relations (A.2)-(A.9), free energy (A.1) is written as

$$\begin{aligned} f &= \frac{1}{N^2} \sum_{l, l'} a_{xx}(l, l') \sum_{\alpha}^{x, y, z} m_{l\alpha} m_{l'\alpha} \\ &+ \frac{1}{N^4} \sum_{l, l', l'', l'''} \left[ b_{xxxx}(l, l', l'', l''') \sum_{\alpha}^{x, y, z} m_{l\alpha} m_{l'\alpha} m_{l''\alpha} m_{l'''\alpha} \right. \\ &+ b_{yyzz}(l, l', l'', l''') \sum_{(\alpha, \beta)}^{(y, z)(z, x)(x, y)} (m_{l\alpha} m_{l'\alpha} m_{l''\beta} m_{l'''\beta} \\ &\quad + m_{l\beta} m_{l'\beta} m_{l''\alpha} m_{l'''\alpha}) \\ &+ b_{yzyy}(l, l', l'', l''') \sum_{(\alpha, \beta)}^{(y, z)(z, x)(x, y)} (m_{l\alpha} m_{l'\beta} m_{l''\beta} m_{l'''\alpha} \\ &\quad + m_{l\beta} m_{l'\alpha} m_{l''\alpha} m_{l'''\beta}) \\ &\left. + b_{yzyz}(l, l', l'', l''') \sum_{(\alpha, \beta)}^{(y, z)(z, x)(x, y)} (m_{l\alpha} m_{l'\beta} m_{l''\alpha} m_{l'''\beta} \right. \\ &\quad \left. + m_{l\beta} m_{l'\alpha} m_{l''\beta} m_{l'''\alpha}) \right]. \quad (\text{A}\cdot 10) \end{aligned}$$

By grouping the same fourth-order terms of  $\{m_{l\alpha}\}$  in the summations with respect to site indices, we have

$$\begin{aligned} f &= \frac{1}{N^2} \sum_{l, l'} a_{xx}(l, l') \sum_{\alpha}^{x, y, z} m_{l\alpha} m_{l'\alpha} \\ &+ \frac{1}{N^4} \sum_{l, l', l'', l'''} \left[ b_{xxxx}(l, l', l'', l''') \sum_{\alpha}^{x, y, z} m_{l\alpha} m_{l'\alpha} m_{l''\alpha} m_{l'''\alpha} \right. \\ &\left. + \{b_{yyzz}(l, l', l'', l''') + b_{yzyy}(l, l'', l''', l') + b_{yzyz}(l, l'', l', l''')\} \right] \end{aligned}$$

$$\begin{aligned} &\times \sum_{(\alpha, \beta)}^{(y, z)(z, x)(x, y)} (m_{l\alpha} m_{l'\alpha} m_{l''\beta} m_{l'''\beta} \\ &\quad + m_{l\beta} m_{l'\beta} m_{l''\alpha} m_{l'''\alpha}). \quad (\text{A}\cdot 11) \end{aligned}$$

Thus we reach eq. (2.2).

In order to obtain the expression for an isotropic system which is invariant under any rotation of magnetic moments, it is sufficient to require that free energy (2.2) be invariant with respect to the  $\pi/4$  rotation of magnetic moments about the  $z$  axis:

$$\begin{aligned} &f(\{m_{lx}\}, \{m_{ly}\}, \{m_{lz}\}) \\ &= f\left(\left\{\frac{1}{\sqrt{2}}(m_{lx} - m_{ly})\right\}, \left\{\frac{1}{\sqrt{2}}(m_{lx} + m_{ly})\right\}, \{m_{lz}\}\right). \quad (\text{A}\cdot 12) \end{aligned}$$

This yields the relation  $C(l, l', l'', l''') \equiv b_{yyzz}(l, l', l'', l''') + b_{yzyy}(l, l'', l''', l') + b_{yzyz}(l, l'', l', l''') - b_{xxxx}(l, l', l'', l''') = 0$ . The resulting free energy satisfies the rotational invariance and thus describes the free energy for the isotropic system.

## Appendix B: Expression of Free Energy with Three Wave Vectors

The phenomenological free energy for fcc crystals is given by eq. (2.4) in §2 for the general  $\mathbf{q}$  vectors. In this appendix we derive the expression of the free energy for SDWs consisting of three wave vectors,  $\mathbf{Q}_1$ ,  $\mathbf{Q}_2$ , and  $\mathbf{Q}_3$ .

### B.1 Commensurate case

We consider here the SDW structures having commensurate wave vectors

$$\begin{aligned} \hat{\mathbf{Q}}_1 &= (1, 0, 0)2\pi/a, & \hat{\mathbf{Q}}_2 &= (0, 1, 0)2\pi/a, \\ & & \hat{\mathbf{Q}}_3 &= (0, 0, 1)2\pi/a. \quad (\text{B}\cdot 1) \end{aligned}$$

The magnetic moment vectors  $\mathbf{m}(\hat{\mathbf{Q}}_1)$ ,  $\mathbf{m}(\hat{\mathbf{Q}}_2)$ , and  $\mathbf{m}(\hat{\mathbf{Q}}_3)$  are real and orthogonal to each other:

$$\mathbf{m}(\hat{\mathbf{Q}}_2) \cdot \mathbf{m}(\hat{\mathbf{Q}}_3) = \mathbf{m}(\hat{\mathbf{Q}}_3) \cdot \mathbf{m}(\hat{\mathbf{Q}}_1) = \mathbf{m}(\hat{\mathbf{Q}}_1) \cdot \mathbf{m}(\hat{\mathbf{Q}}_2) = 0. \quad (\text{B}\cdot 2)$$

The free energy having three wave vectors can be written with the help of eq. (2.4). Using relations (B.1) and (B.2), we reach

$$\begin{aligned} f_{\text{co}} &= 4 \sum_{i=1}^3 [A(\hat{\mathbf{Q}}_i) |\mathbf{m}(\hat{\mathbf{Q}}_i)|^2 \\ &\quad + (B_1(\hat{\mathbf{Q}}_i) + \tilde{B}_2(\hat{\mathbf{Q}}_i)) |\mathbf{m}(\hat{\mathbf{Q}}_i)|^4] \\ &\quad + \sum_{(i, j)}^{(2, 3)(3, 1)(1, 2)} \tilde{B}_3(\hat{\mathbf{Q}}_i, \hat{\mathbf{Q}}_j) |\mathbf{m}(\hat{\mathbf{Q}}_i)|^2 |\mathbf{m}(\hat{\mathbf{Q}}_j)|^2. \quad (\text{B}\cdot 3) \end{aligned}$$

The coefficients  $B_1(\hat{\mathbf{Q}}_i)$ ,  $\tilde{B}_2(\hat{\mathbf{Q}}_i)$ , and  $\tilde{B}_3(\hat{\mathbf{Q}}_i, \hat{\mathbf{Q}}_j)$  are defined as follows:

$$B_1(\hat{\mathbf{Q}}_i) \equiv \sum_{\mathbf{p}} B(\{\hat{\mathbf{Q}}_i, -\hat{\mathbf{Q}}_i\}, \{\hat{\mathbf{Q}}_i, -\hat{\mathbf{Q}}_i\}) \quad (i = 1, 2, 3), \quad (\text{B}\cdot 4)$$

$$\begin{aligned} \tilde{B}_2(\hat{\mathbf{Q}}_i) &\equiv B(\hat{\mathbf{Q}}_i, \hat{\mathbf{Q}}_i, \hat{\mathbf{Q}}_i, \hat{\mathbf{Q}}_i) \\ &\quad + B(-\hat{\mathbf{Q}}_i, -\hat{\mathbf{Q}}_i, -\hat{\mathbf{Q}}_i, -\hat{\mathbf{Q}}_i) \\ &\quad + \sum_{\mathbf{p}} \left[ B(\{(\hat{\mathbf{Q}}_i, \hat{\mathbf{Q}}_i), (-\hat{\mathbf{Q}}_i, -\hat{\mathbf{Q}}_i)\}) \right. \\ &\quad \left. + B(\{(\hat{\mathbf{Q}}_i, \hat{\mathbf{Q}}_i), \{\hat{\mathbf{Q}}_i, -\hat{\mathbf{Q}}_i\}\}) \right. \\ &\quad \left. + B(\{(-\hat{\mathbf{Q}}_i, -\hat{\mathbf{Q}}_i), \{\hat{\mathbf{Q}}_i, -\hat{\mathbf{Q}}_i\}\}) \right] \quad (i = 1, 2, 3), \quad (\text{B}\cdot 5) \end{aligned}$$

$$\begin{aligned} \tilde{B}_3(\hat{\mathbf{Q}}_i, \hat{\mathbf{Q}}_j) &\equiv \sum_{\mathbf{p}} \left[ B(\{\{\hat{\mathbf{Q}}_i, -\hat{\mathbf{Q}}_i\}, \{\hat{\mathbf{Q}}_j, -\hat{\mathbf{Q}}_j\}\}) \right. \\ &\quad + B(\{(\hat{\mathbf{Q}}_i, \hat{\mathbf{Q}}_i), \{\hat{\mathbf{Q}}_j, -\hat{\mathbf{Q}}_j\}\}) \\ &\quad + B(\{(-\hat{\mathbf{Q}}_i, -\hat{\mathbf{Q}}_i), \{\hat{\mathbf{Q}}_j, -\hat{\mathbf{Q}}_j\}\}) \\ &\quad + B(\{\{\hat{\mathbf{Q}}_i, -\hat{\mathbf{Q}}_i\}, (\hat{\mathbf{Q}}_j, \hat{\mathbf{Q}}_j)\}) \\ &\quad + B(\{\{\hat{\mathbf{Q}}_i, -\hat{\mathbf{Q}}_i\}, (-\hat{\mathbf{Q}}_j, -\hat{\mathbf{Q}}_j)\}) \\ &\quad + B(\{(\hat{\mathbf{Q}}_i, \hat{\mathbf{Q}}_i), (\hat{\mathbf{Q}}_j, \hat{\mathbf{Q}}_j)\}) \\ &\quad + B(\{(-\hat{\mathbf{Q}}_i, -\hat{\mathbf{Q}}_i), (-\hat{\mathbf{Q}}_j, -\hat{\mathbf{Q}}_j)\}) \\ &\quad + B(\{(\hat{\mathbf{Q}}_i, \hat{\mathbf{Q}}_i), (-\hat{\mathbf{Q}}_j, -\hat{\mathbf{Q}}_j)\}) \\ &\quad \left. + B(\{(-\hat{\mathbf{Q}}_i, -\hat{\mathbf{Q}}_i), (\hat{\mathbf{Q}}_j, \hat{\mathbf{Q}}_j)\}) \right] \\ &\quad ((i, j) = (2, 3)(3, 1)(1, 2)). \quad (\text{B}\cdot 6) \end{aligned}$$

In eqs. (B·4)-(B·6) and below,  $\sum_{\mathbf{p}}$  denotes summations with respect to all the permutations of elements in the curly brackets. Wherever a parenthesis or curly bracket appears, it is regarded as one element when counting permutation.

Since the wave vectors  $\hat{\mathbf{Q}}_1$ ,  $\hat{\mathbf{Q}}_2$ , and  $\hat{\mathbf{Q}}_3$  are all equivalent on the fcc lattice, it follows that

$$\tilde{A}_Q \equiv 4A(\hat{\mathbf{Q}}_1) = 4A(\hat{\mathbf{Q}}_2) = 4A(\hat{\mathbf{Q}}_3), \quad (\text{B}\cdot 7)$$

$$B_{1Q} \equiv B_1(\hat{\mathbf{Q}}_1) = B_1(\hat{\mathbf{Q}}_2) = B_1(\hat{\mathbf{Q}}_3), \quad (\text{B}\cdot 8)$$

$$\tilde{B}_{2Q} \equiv \tilde{B}_2(\hat{\mathbf{Q}}_1) = \tilde{B}_2(\hat{\mathbf{Q}}_2) = \tilde{B}_2(\hat{\mathbf{Q}}_3), \quad (\text{B}\cdot 9)$$

$$\tilde{B}_{1QQ} \equiv \tilde{B}_3(\hat{\mathbf{Q}}_2, \hat{\mathbf{Q}}_3) = \tilde{B}_3(\hat{\mathbf{Q}}_3, \hat{\mathbf{Q}}_1) = \tilde{B}_3(\hat{\mathbf{Q}}_1, \hat{\mathbf{Q}}_2). \quad (\text{B}\cdot 10)$$

With the use of relations (B·7)-(B·10), free energy (B·3) is expressed as

$$\begin{aligned} f_{\text{co}} &= \sum_{i=1}^3 [\tilde{A}_Q |\mathbf{m}(\hat{\mathbf{Q}}_i)|^2 + (B_{1Q} + \tilde{B}_{2Q}) |\mathbf{m}(\hat{\mathbf{Q}}_i)|^4] \\ &\quad + \sum_{(i,j)}^{(2,3)(3,1)(1,2)} \tilde{B}_{1QQ} |\mathbf{m}(\hat{\mathbf{Q}}_i)|^2 |\mathbf{m}(\hat{\mathbf{Q}}_j)|^2. \quad (\text{B}\cdot 11) \end{aligned}$$

This is the free energy for the commensurate case given by eq. (3.10) in §3.

### B.2 Incommensurate case

In the incommensurate case, we consider three equivalent wave vectors,  $\mathbf{Q}_1$ ,  $\mathbf{Q}_2$ , and  $\mathbf{Q}_3$ , which satisfy incommensurate conditions (4.41)-(4.43) in §4. Using expression (2.4), the free energy having three incommensurate wave vectors can be written as follows:

$$\begin{aligned} f_{\text{ic}} &= \sum_{i=1}^3 [2A(\mathbf{Q}_i) |\mathbf{m}(\mathbf{Q}_i)|^2 + B_1(\mathbf{Q}_i) |\mathbf{m}(\mathbf{Q}_i)|^4 \\ &\quad + B_2(\mathbf{Q}_i) \mathbf{m}^2(\mathbf{Q}_i) \mathbf{m}^{*2}(\mathbf{Q}_i)] \\ &\quad + \sum_{(i,j)}^{(2,3)(3,1)(1,2)} [B_1(\mathbf{Q}_i, \mathbf{Q}_j) |\mathbf{m}(\mathbf{Q}_i)|^2 |\mathbf{m}(\mathbf{Q}_j)|^2 \\ &\quad + B_2(\mathbf{Q}_i, \mathbf{Q}_j) |\mathbf{m}(\mathbf{Q}_i) \cdot \mathbf{m}(\mathbf{Q}_j)|^2 \\ &\quad + B_3(\mathbf{Q}_i, \mathbf{Q}_j) |\mathbf{m}(\mathbf{Q}_i) \cdot \mathbf{m}^*(\mathbf{Q}_j)|^2]. \quad (\text{B}\cdot 12) \end{aligned}$$

Here, the coefficients  $B_1(\mathbf{Q}_i)$ ,  $B_2(\mathbf{Q}_i)$  ( $i = 1, 2, 3$ ),  $B_1(\mathbf{Q}_i, \mathbf{Q}_j)$ ,  $B_2(\mathbf{Q}_i, \mathbf{Q}_j)$ , and  $B_3(\mathbf{Q}_i, \mathbf{Q}_j)$  ( $(i, j) = (2, 3)(3, 1)(1, 2)$ ) are defined as follows:

$$B_1(\mathbf{Q}_i) \equiv \sum_{\mathbf{p}} B(\{\mathbf{Q}_i, -\mathbf{Q}_i\}, \{\mathbf{Q}_i, \mathbf{Q}_i\}) \quad (i = 1, 2, 3), \quad (\text{B}\cdot 13)$$

$$B_2(\mathbf{Q}_i) \equiv \sum_{\mathbf{p}} B(\{(\mathbf{Q}_i, \mathbf{Q}_i), (-\mathbf{Q}_i, -\mathbf{Q}_i)\}) \quad (i = 1, 2, 3), \quad (\text{B}\cdot 14)$$

$$B_1(\mathbf{Q}_i, \mathbf{Q}_j) \equiv \sum_{\mathbf{p}} B(\{\{\mathbf{Q}_i, -\mathbf{Q}_i\}, \{\mathbf{Q}_j, -\mathbf{Q}_j\}\}) \\ ((i, j) = (2, 3)(3, 1)(1, 2)), \quad (\text{B}\cdot 15)$$

$$B_2(\mathbf{Q}_i, \mathbf{Q}_j) \equiv \sum_{\mathbf{p}} B(\{\{\mathbf{Q}_i, \mathbf{Q}_j\}, \{-\mathbf{Q}_i, -\mathbf{Q}_j\}\}) \\ ((i, j) = (2, 3)(3, 1)(1, 2)), \quad (\text{B}\cdot 16)$$

$$B_3(\mathbf{Q}_i, \mathbf{Q}_j) \equiv \sum_{\mathbf{p}} B(\{\{\mathbf{Q}_i, -\mathbf{Q}_j\}, \{-\mathbf{Q}_i, \mathbf{Q}_j\}\}) \\ ((i, j) = (2, 3)(3, 1)(1, 2)). \quad (\text{B}\cdot 17)$$

Since the wave vectors  $\mathbf{Q}_1$ ,  $\mathbf{Q}_2$ , and  $\mathbf{Q}_3$  are all equivalent in the fcc lattice, it follows that

$$A_Q \equiv 2A(\mathbf{Q}_1) = 2A(\mathbf{Q}_2) = 2A(\mathbf{Q}_3), \quad (\text{B}\cdot 18)$$

$$B_{1Q} \equiv B_1(\mathbf{Q}_1) = B_1(\mathbf{Q}_2) = B_1(\mathbf{Q}_3), \quad (\text{B}\cdot 19)$$

$$B_{2Q} \equiv B_2(\mathbf{Q}_1) = B_2(\mathbf{Q}_2) = B_2(\mathbf{Q}_3), \quad (\text{B}\cdot 20)$$

$$B_{1QQ} \equiv B_1(\mathbf{Q}_2, \mathbf{Q}_3) = B_1(\mathbf{Q}_3, \mathbf{Q}_1) = B_1(\mathbf{Q}_1, \mathbf{Q}_2), \quad (\text{B}\cdot 21)$$

$$B_{2QQ} \equiv B_2(\mathbf{Q}_2, \mathbf{Q}_3) = B_2(\mathbf{Q}_3, \mathbf{Q}_1) = B_2(\mathbf{Q}_1, \mathbf{Q}_2), \quad (\text{B}\cdot 22)$$

$$B_{3QQ} \equiv B_3(\mathbf{Q}_2, \mathbf{Q}_3) = B_3(\mathbf{Q}_3, \mathbf{Q}_1) = B_3(\mathbf{Q}_1, \mathbf{Q}_2). \quad (\text{B}\cdot 23)$$

With the use of relations (B-18)-(B-23), free energy (B-12) is expressed as

$$f_{ic} = \sum_{i=1}^3 [A_Q |\mathbf{m}(\mathbf{Q}_i)|^2 + B_{1Q} |\mathbf{m}(\mathbf{Q}_i)|^4 + B_{2Q} \mathbf{m}^2(\mathbf{Q}_i) \mathbf{m}^{*2}(\mathbf{Q}_i)] + \sum_{(i,j)}^{(2,3)(3,1)(1,2)} [B_{1QQ} |\mathbf{m}(\mathbf{Q}_i)|^2 |\mathbf{m}(\mathbf{Q}_j)|^2 + B_{2QQ} |\mathbf{m}(\mathbf{Q}_i) \cdot \mathbf{m}(\mathbf{Q}_j)|^2 + B_{3QQ} |\mathbf{m}(\mathbf{Q}_i) \cdot \mathbf{m}^*(\mathbf{Q}_j)|^2]. \quad (\text{B}\cdot 24)$$

This is the free energy for the incommensurate case, eq. (4.44), in §4.

- 1) E. Fawcett: Rev. Mod. Phys. **60** (1988) 209.
- 2) T. Yamada: J. Phys. Soc. Jpn. **28** (1970) 596.
- 3) T. Yamada, N. Kunitomi, and Y. Nakai: J. Phys. Soc. Jpn. **30** (1971) 1614.
- 4) D. Meneghetti and S. S. Sidhu: Phys. Rev. **105** (1957) 130.
- 5) Y. Tsunoda: J. Phys.: Condens. Matter **1** (1989) 10427.
- 6) D. Qian, X. F. Jin, J. Barthel, M. Klaua and J. Kirschner: Phys. Rev. Lett. **87** (2001) 227204.
- 7) G. E. Bacon, I. W. Dunmur, J. H. Smith and R. Street: Proc. Roy. Soc. (London) A **241** (1957) 223.
- 8) H. Uchishiba, T. Hori and Y. Nakagawa: J. Phys. Soc. Jpn. **28** (1970) 792.
- 9) Y. Endoh and Y. Ishikawa: J. Phys. Soc. Jpn. **30** (1971) 1614.
- 10) R. Yamauchi, T. Hori, M. Miyakawa and K. Fukamichi: J. Alloys Comp. **309** (2000) 16.
- 11) S. Akbar, Y. Kakehashi and N. Kimura: J. Phys.: Condens. Matter **10** (1998) 2081.
- 12) R. S. Fishman and S. H. Liu: Phys. Rev. B **59** (1999) 8672.
- 13) Y. Kakehashi, S. Akbar and N. Kimura: in *Itinerant Electron Magnetism: Fluctuation Effects & Critical Phenomena*, ed. D. Wagner, W. Braunek and A. Solontsov, NATO Science Series: 3. High Technology (Kluwer Academic, Netherlands, 1998), Vol. 55, pp. 193-228.
- 14) S. C. Abrahams, L. Guttman and J. S. Kasper: Phys. Rev. **127** (1962) 2052.
- 15) U. Gradmann and H. O. Isbert: J. Magn. Magn. Mater. **15-8** (1980) 1109.
- 16) D. Pescia, M. Stampanoni, G. L. Bona, A. Vaterlaus, R. F. Willis and F. Meier: Phys. Rev. Lett. **58** (1987) 2126.
- 17) W. A. A. Macedo and W. Keune: Phys. Rev. Lett. **61** (1988) 475.
- 18) Dongqi Li, M. Freitag, J. Pearson, Z. Q. Qiu and S. D. Bader: Phys. Rev. Lett. **72** (1994) 3112.
- 19) J. W. Freeland, I. L. Grigorov and J. C. Walker: Phys. Rev. B **57** (1988) 80.
- 20) O. N. Mryasov, A. I. Liechtenstein, L. M. Sandratskii and V. A. Gubanov: J. Phys.: Condens. Matter **3** (1991) 7683.
- 21) M. Uhl, L. M. Sandratskii and J. Kübler: J. Magn. Magn. Mater. **103** (1992) 314.
- 22) M. Körling and J. Ergon: Phys. Rev. B **54** (1996) R8293.
- 23) D. M. Bylander and L. Kleinman: Phys. Rev. B **58** (1998) 9207.
- 24) D. M. Bylander and L. Kleinman: Phys. Rev. B **59** (1999) 6278.
- 25) D. M. Bylander and L. Kleinman: Phys. Rev. B **60** (1999) R9916.
- 26) K. Knöpfle, L. M. Sandratskii and J. Kübler: Phys. Rev. B **62** (2000) 5564.
- 27) E. Sjöstedt and L. Nordström: Phys. Rev. B **66** (2002) 014447.
- 28) S. Fujii, S. Ishida and S. Asano: J. Phys. Soc. Jpn. **60** (1991) 4300.
- 29) V. P. Antropov, M. I. Katsnelson, M. van Schilfgaarde and B. N. Harmon: Phys. Rev. Lett. **75** (1995) 729.
- 30) V. P. Antropov, M. I. Katsnelson, B. N. Harmon, M. van Schilfgaarde and D. Kusnezov: Phys. Rev. B **54** (1996) 1019.
- 31) Y. Kakehashi, S. Akbar and N. Kimura: Phys. Rev. B **57** (1998) 8354.
- 32) Y. Kakehashi and N. Kimura: Phys. Rev. B **60** (1999) 3316.
- 33) Y. Kakehashi, O. Jepsen and N. Kimura: Phys. Rev. B **65** (2002) 134418.
- 34) T. Uchida and Y. Kakehashi: Phys. Status Solidi A **196** (2003) 193.
- 35) T. Uchida and Y. Kakehashi: J. Magn. Magn. Mater. **272-276** (2004) 527.
- 36) M. B. Walker: Phys. Rev. B **22** (1980) 1338.
- 37) Xi. Zhu and M. B. Walker: Phys. Rev. B **34** (1986) 8064.
- 38) T. Jo and K. Hirai: J. Phys. Soc. Jpn. **55** (1986) 2017.
- 39) The phase diagram for the commensurate case was presented in Fig. 1 in ref. 34 for different combinations of the expansion coefficients, where the region "NM" should be read as "Other structures".
- 40) J. S. Kouvel and J. S. Kasper: J. Phys. Chem. Solids **24** (1963) 529.
- 41) A. Yoshimori: J. Phys. Soc. Jpn. **14** (1959) 807.
- 42) T. A. Kaplan: Phys. Rev. **116** (1959) 888.
- 43) T. A. Kaplan: Phys. Rev. **119** (1960) 1460.
- 44) The phase diagram allowing for the  $1\mathbf{Q}$  helical and  $1\mathbf{Q}$ ,  $2\mathbf{Q}$ ,  $3\mathbf{Q}$  linear SDWs was presented in Fig. 2 in ref. 34 for different combinations of the expansion coefficients, where the region "NM" should be read as "Other structures".
- 45) T. Naono and Y. Tsunoda: J. Phys.: Condens. Matter **16** (2004) 7723.